

# Lawrence Berkeley National Laboratory

## Recent Work

### Title

Reactions of Barium Atoms with Triatomic Oxidants. I. Ba + NO(2)(1)

### Permalink

<https://escholarship.org/uc/item/0tz7j5rm>

### Journal

Journal of Chemical Physics, 96(9)

### Authors

Davis, H.F.

Suits, Arthur G.

Lee, Yuan T.

### Publication Date

1991-11-01



# Lawrence Berkeley Laboratory

UNIVERSITY OF CALIFORNIA

## Materials & Chemical Sciences Division

Submitted to Journal of Chemical Physics

### Reactions of Barium Atoms with Triatomic Oxidants 1: Ba + NO<sub>2</sub><sup>1</sup>

H.F. Davis, A.G. Suits, and Y.T. Lee

November 1991

*U. C. Lawrence Berkeley Laboratory  
Library, Berkeley*

**FOR REFERENCE**

Not to be taken from this room



Bldg. 50 Library.  
Copy 1

LBL-31492

### DISCLAIMER

This document was prepared as an account of work sponsored by the United States Government. Neither the United States Government nor any agency thereof, nor The Regents of the University of California, nor any of their employees, makes any warranty, express or implied, or assumes any legal liability or responsibility for the accuracy, completeness, or usefulness of any information, apparatus, product, or process disclosed, or represents that its use would not infringe privately owned rights. Reference herein to any specific commercial product, process, or service by its trade name, trademark, manufacturer, or otherwise, does not necessarily constitute or imply its endorsement, recommendation, or favoring by the United States Government or any agency thereof, or The Regents of the University of California. The views and opinions of authors expressed herein do not necessarily state or reflect those of the United States Government or any agency thereof or The Regents of the University of California and shall not be used for advertising or product endorsement purposes.

Lawrence Berkeley Laboratory is an equal opportunity employer.

## **DISCLAIMER**

This document was prepared as an account of work sponsored by the United States Government. While this document is believed to contain correct information, neither the United States Government nor any agency thereof, nor the Regents of the University of California, nor any of their employees, makes any warranty, express or implied, or assumes any legal responsibility for the accuracy, completeness, or usefulness of any information, apparatus, product, or process disclosed, or represents that its use would not infringe privately owned rights. Reference herein to any specific commercial product, process, or service by its trade name, trademark, manufacturer, or otherwise, does not necessarily constitute or imply its endorsement, recommendation, or favoring by the United States Government or any agency thereof, or the Regents of the University of California. The views and opinions of authors expressed herein do not necessarily state or reflect those of the United States Government or any agency thereof or the Regents of the University of California.

**REACTIONS OF BARIUM ATOMS WITH TRIATOMIC OXIDANTS. 1: Ba + NO<sub>2</sub><sup>1</sup>**

H. Floyd Davis, Arthur G. Suits, and Yuan T. Lee

Chemical Sciences Division  
Lawrence Berkeley Laboratory and  
Department of Chemistry  
University of California  
Berkeley CA 94720

November 1991

This work was supported by the Director, Office of Energy Research, Office of Basic Energy Sciences, Chemical Sciences Division, of the U.S. Department of Energy under Contract No. DE-AC03-76SF00098.

**REACTIONS OF BARIUM ATOMS WITH TRIATOMIC OXIDANTS. 1: Ba + NO<sub>2</sub><sup>1</sup>****ABSTRACT**

Angular and velocity distributions of the neutral products resulting from the reaction Ba + NO<sub>2</sub> were measured using the crossed molecular beams method. Despite a large reaction exoergicity ( $\Delta H = -61$  kcal/mole), formation of the dominant ground state BaO(<sup>1</sup>Σ) + NO products results primarily from decay of long-lived Ba<sup>+</sup>NO<sub>2</sub><sup>-</sup> collision complexes, even at incident collision energies as high as 59 kcal/mole or with electronic excitation of the Ba atom. A large fraction of the reaction exoergicity is channeled into product translational energy. This rather unusual behavior results from a large exit potential energy barrier for decay of the initially formed singly ionic Ba<sup>+</sup>NO<sub>2</sub><sup>-</sup> intermediate to ground state doubly ionic Ba<sup>2+</sup>O<sup>2-</sup>. A secondary source of forward scattered, internally excited BaO results from a direct reaction without the involvement of long-lived intermediates. An additional minor channel, formation of BaNO + O is observed from ground state Ba + NO<sub>2</sub> at high collision energies by a direct reaction mechanism. Unlike the dominant BaO + NO channel which involves harpooning at the first ionic-covalent curve crossing, formation of BaNO from reaction of ground state Ba likely results from the small range of collision geometries which are able to avoid long range electron transfer. The BaNO + O channel was enhanced substantially by electronic excitation of the incident barium atom. However, BaNO from reactions of electronically excited Ba primarily resulted from decay of collision complexes, rather than from a direct mechanism.

## I. INTRODUCTION

The early studies by Michael Polanyi and coworkers<sup>2</sup> on the reactions of alkali metal atoms with halogen containing molecules in diffusion flames initiated a field of research that has led to profound insight into the reactions of monovalent species. The early observation that reaction rates were larger than those expected by gas kinetic theory led to the now famous "harpoon mechanism"<sup>2,3</sup> used to describe the general class of reactions initiated by long range electron transfer.<sup>4</sup> In the 60's the advancement of crossed molecular beams techniques confirmed these early ideas and led to a detailed understanding of the reaction dynamics of monovalent atoms.<sup>5,6</sup> In the reaction  $K + Br_2 \rightarrow KBr + Br$ , the facile dissociation of newly formed diatomic halogen anions<sup>7</sup> under the influence of alkali cations led to the "spectator stripping" mechanism with the product salt molecule forward scattered with respect to the incoming alkali atom. On the other hand, the pronounced backscattering of the KI product from the reaction  $K + CH_3I$ <sup>8</sup> resulted from the need for approach of the alkali atom towards the halogen end of the molecule, followed by strong repulsive forces in the exit channel. These two prototype reactions illustrated two extremes in chemical dynamics.

Although most early studies were restricted to alkali atoms due to the ease of product detection using surface ionization,<sup>9</sup> the development of the "universal" crossed molecular beams apparatus<sup>10</sup> and optical techniques such as laser induced fluorescence<sup>11</sup> and chemiluminescence detection<sup>12</sup> permitted studies of a variety of other neutral atom-molecule reactions. More than two decades ago, BaO chemiluminescence was first observed from single collisions between Ba atoms and oxygen-containing triatomic molecules.<sup>13-15</sup> Due to the potential applications of these systems in the development of electronic transition chemical lasers, these and many subsequent studies focussed on the identification and relative yields of nascent chemiluminescent species. Although hopes for practical laser applications soon faded, fascination with the reactions continued primarily because the origin of the BaO emission spectrum was not well understood.<sup>16,17</sup> In most cases, the chemiluminescence yield was found to be pressure dependent: increasing pressure led to increased chemiluminescence. More than 50 papers<sup>16</sup> were devoted to

these studies but most focussed on Ba + N<sub>2</sub>O since the effect in that case was particularly dramatic--the chemiluminescence yield increased from 2.5% to 20% upon increasing the pressure from 1x10<sup>-4</sup> Torr to 10 Torr.

There has been considerably less work devoted to the reaction Ba + NO<sub>2</sub>, primarily because of the small photon yield. It was found that more than 98% of all BaO was formed in non-chemiluminescent states.<sup>16,17</sup> Careful measurements by several groups showed that the collision free yield of chemiluminescent BaO(A<sup>1</sup>Σ<sup>+</sup>) molecules was only 0.2%, with the value reaching a maximum of ≤2% at high pressure. According to Hsu and Pruett<sup>17</sup>, the very low high pressure yield could be attributed to the fact that the nascent BaO from Ba + NO<sub>2</sub> are almost all formed in the X<sup>1</sup>Σ ground state with only a small amount of vibrational energy. This dominant ground state BaO possessed insufficient internal energy for electronic excitation by secondary collisions.

Angular distributions of the BaO resulting from Ba + NO<sub>2</sub> were measured by Haberman, et al.<sup>18</sup> These experiments were rather primitive by present standards, employing effusive beams with broad beam velocity distributions, and no product velocity distributions could be obtained. They concluded that the BaO product was forward scattered with respect to the Ba beam with only a small fraction of the available energy appearing in BaO-NO translational recoil. Herm and coworkers,<sup>19</sup> using a similar apparatus studied the reactions of Sr and Ca (but not Ba) with NO<sub>2</sub>. Their results on the lighter alkaline earth species were consistent with the results of Haberman on Ba + NO<sub>2</sub>. Based on the work from these two laboratories, it was concluded that the reactions of alkaline earth atoms with NO<sub>2</sub> were analogous to the well-studied alkali-halogen systems.<sup>7,20</sup> Due to the low ionization potential of Ba (5.2eV)<sup>21</sup> and large electron affinity of NO<sub>2</sub> (2.3eV)<sup>22</sup>, the reaction is initiated by long range electron transfer,<sup>4,13-15</sup> consistent with a very large experimentally determined reaction cross section (>150Å<sup>2</sup>).<sup>13</sup> By analogy with the alkali-halogen systems, it was argued that after long range electron transfer, the strong field of the approaching Ba<sup>+</sup> led to immediate dissociation of NO<sub>2</sub><sup>-</sup>. The incoming Ba<sup>+</sup> "picked up" the O<sup>-</sup> ion with the newly formed BaO molecule continuing in nearly the same center-of-mass (CM) direction as the incident Ba atom<sup>18,19</sup>.

This direct reaction mechanism contrasted the general behavior seen earlier by Ham and Kinsey<sup>23</sup> in scattering of alkali atoms such as Cs with SO<sub>2</sub>, CO<sub>2</sub> and NO<sub>2</sub>. Angular distributions measured using a surface ionization detector provided good evidence that collisions between alkali atoms and these triatomic oxidants led to formation of strongly bound ionic collision complexes (e.g. Cs<sup>+</sup>SO<sub>2</sub><sup>-</sup>). The center-of-mass angular distributions of the nonreactively scattered Cs showed forward-backward symmetry, indicating that the lifetime of the ionic intermediate exceeded several rotational periods.<sup>24</sup> Decay of a long-lived prolate collision complex is expected to result in a center-of-mass product angular distribution peaking at  $\theta_{\text{CM}} = 0^\circ$  and  $180^\circ$ ; this often leads to a characteristic laboratory angular distribution exhibiting two peaks. In the case of SO<sub>2</sub> and CO<sub>2</sub>, chemical reaction was too endoergic to be possible; the observed Cs signal could only result from decay of complexes back to reactants. Although the reaction Cs + NO<sub>2</sub> → CsO + NO was thought to be slightly exoergic, it was not clear from that work whether or not a reaction actually occurred. Subsequently, Herm and Herschbach<sup>25</sup> observed formation of CsO with a large cross section from Cs + NO<sub>2</sub>. The bimodal character of the observed CsO laboratory angular distribution was again strongly suggestive of the participation of long-lived Cs<sup>+</sup>NO<sub>2</sub><sup>-</sup> reaction intermediates. However, they resisted drawing any definite conclusions because uncertainties remained in the analysis of the data for the reactive channel since the product translational energy distributions were not recorded. We have recently measured angular and velocity distributions for the reaction Na + NO<sub>2</sub> → NaO + NO using supersonic beams in our apparatus.<sup>27</sup> We observe strong NaO signal from decay of long-lived Na<sup>+</sup>NO<sub>2</sub><sup>-</sup> intermediates. Based on this and the past nonreactive and reactive scattering results, there is little doubt that reaction of the heavier alkalis including Cs + NO<sub>2</sub> involve long-lived reaction intermediates.<sup>28</sup>

That alkalis react with NO<sub>2</sub> by formation of long-lived complexes is not surprising since the reactions are nearly thermoneutral, NO<sub>2</sub><sup>-</sup> is a stable ion, and the ion pair Cs<sup>+</sup>NO<sub>2</sub><sup>-</sup> has a deep potential well. The conclusion that alkaline earth atoms react by a direct stripping mechanism, however, also seems very reasonable. The Ba<sup>+</sup>NO<sub>2</sub><sup>-</sup> and Cs<sup>+</sup>NO<sub>2</sub><sup>-</sup> singly charged ionic intermediates are expected to be similar; both should be bound by about 65 kcal/mole with respect to reactants.<sup>25,26</sup> However, the reaction exoergicities are widely different: Ba + NO<sub>2</sub> → BaO + NO is highly exoergic-  $\Delta H = -61$  kcal/mole<sup>30</sup> (Table I), whereas Cs + NO<sub>2</sub> → CsO + NO is

now known to be slightly endoergic ( $\Delta H=+2$  kcal/mole).<sup>30</sup> The large difference is due to the divalent nature of barium: the ground state BaO molecule, best described as  $Ba^{2+}O^{2-}$ <sup>31</sup> is bound by 133 kcal/mole, whereas the  $Cs^+O^-$  binding energy is about half this value (70 kcal/mole).<sup>30</sup> Based on thermodynamics alone, the large exoergicity of the Ba reaction is expected to lead to subpicosecond lifetimes for  $Ba^+NO_2^-$ <sup>32</sup> with the BaO forward scattered; whereas the slight endoergicity of the reaction of cesium allows the  $Cs^+NO_2^-$  reaction intermediate to survive many rotational periods before decaying to products or back to reactants.

Although velocity distributions were not measured in the previous alkaline earth +  $NO_2$  crossed beams experiments, based on the product angular distributions it was concluded that the nascent products were formed with relatively low translational energy.<sup>18,19</sup> The more recent laser induced fluorescence work<sup>17</sup> indicated that the dominant ground state BaO was vibrationally cold. The following question arises: Where has the 61 kcal/mole reaction exoergicity been disposed? For a reaction apparently involving long range electron transfer with immediate dissociation of  $NO_2^-$ , there is no obvious reason why the reaction exoergicity should be exclusively channeled into vibrational excitation of the NO product. Although it is known that the products are rotationally hot, it seems impossible to believe that so much energy could be preferentially funneled into rotation without the accompanying release of some of the excess energy into translation.

The goal of the present work is to probe the dynamics of the reactions of a divalent metal atom with oxygen containing molecules under single collision conditions. Barium was deemed to be the most suitable alkaline earth atom for several reasons. Owing to its relatively low second ionization potential (10eV)<sup>21</sup> it is most likely to exhibit dynamical effects resulting from its divalency. Also, the first optically allowed electronic transition from the ground state ( $^1P \leftarrow ^1S$ ) is at a wavelength convenient to  $Ar^+$  laser pumped ring dye lasers whereas transitions for the lighter alkaline earths are at less accessible, shorter wavelengths.<sup>33</sup> Here we report on the reaction  $Ba + NO_2$ , and a second paper will focus on  $Ba + ClO_2$  and  $O_3$ .<sup>34a</sup> Although all three triatomic molecules are closely related, the behavior of each provides considerable insight into the reaction dynamics of divalent systems. Unlike all experiments undertaken to date, both the angular and velocity distributions of the products have been measured. Both beams are much

better defined than in the past work from other laboratories, having a narrow velocity distribution characteristic of a supersonic expansion. Our results indicate that previous conclusions, that the  $\text{Ba} + \text{NO}_2$  reaction is analogous to alkali atoms + halogens is not quite correct. We have found that the divalent nature of barium leads to rather interesting and unexpected reaction dynamics.

The primary advantage of the mass spectrometric detection method over chemiluminescence is that all chemical products, including those in the ground electronic states are detected simultaneously. In addition to  $\text{BaO} + \text{NO}$ , a number of other chemical channels are thermodynamically possible from  $\text{Ba} + \text{NO}_2$  (Table I). Mass detection provides the opportunity to observe such products that cannot easily be detected by optical techniques either because of experimental complexities or because their electronic spectrum is unknown. We illustrate this by the observation of  $\text{BaNO}$  in the present experiment. As far as we know, this is the first direct observation of a metal mononitroxide in the gas phase.

## II. EXPERIMENTAL

The universal crossed molecular beams apparatus is shown in Figure 1. A continuous, seeded supersonic beam of barium atoms was formed in a molybdenum oven source with separately heated barium reservoir and nozzle. Details of this source will be published elsewhere.<sup>34b</sup> The barium reservoir was heated to 1050 °C, corresponding to a barium pressure of 10 Torr, and pressurized with 250-700 Torr of an inert gas. The mixture was expanded through a 0.008" diameter nozzle heated to 1350 °C to minimize the formation of clusters. The beam was skimmed by a heated (1000°C) molybdenum skimmer located in the differential pumping region and then collimated to 2° full width by a set of defining slits.

The electronically excited barium atomic beam was produced by optically pumping the  $\text{Ba}(^1\text{P} \leftarrow ^1\text{S})$  resonance either at or upstream of the interaction region using a Coherent 699-21 ring dye laser operating single frequency at 553nm with Rhodamine 560 dye. The fluorescence intensity was continuously monitored during the experiment by imaging the light from the pumped region onto a photomultiplier tube using a commercial telephoto lens. Once the oven was stabilized, the

fluorescence intensity remained constant to within a few percent over a period of several hours.

The metastable  $\text{Ba}(^1\text{D})$  population resulted from radiative decay from the  $^1\text{P}$  state ( $\tau \sim 8.4\text{ns}$ ). By pumping a 1cm length of the beam upstream of the collision zone at 100mW, it was found that 60% of the ground state  $^{138}\text{Ba}$  population was depleted. This measurement was accomplished by splitting off a small portion (10mW) of the laser beam, passing it through an acoustoptic modulator and using the resulting beam to probe the ground state Ba population downstream of the primary pumping region. The 60% fluorescence depletion represents the fractional decrease in ground state population in the beam due to optical pumping to the long lived ( $\sim 1\text{sec}$ ) metastable ( $^1\text{D}$ ) states. This fraction was relatively insensitive to laser power, indicating that the transition was strongly saturated, as was expected at powers above 50mW. Our experiment, together with published<sup>35</sup>  $\text{Ba}(^1\text{P})$  branching ratios indicates that by pumping upstream of the crossing region the  $^{138}\text{Ba}$  in the beam consisted of 45%  $\text{Ba}(^1\text{D})$ , 15%  $\text{Ba}(^3\text{D})$  and 40%  $\text{Ba}(^1\text{S})$ , with all other isotopes in the ground ( $^1\text{S}$ ) state. The reaction of  $\text{Ba}(^1\text{P})$  was studied by focussing the laser to 3mm diameter and pumping at the interaction region. Under these conditions, the  $^{138}\text{Ba}$  consisted of 30%  $\text{Ba}(^1\text{D})$ , 35%  $\text{Ba}(^1\text{P})$  and 35%  $\text{Ba}(^1\text{S})$ . Although the  $\text{Ba}(^1\text{P})$  atoms are well aligned, we have found no orbital alignment dependence for the neutral product channels from  $\text{Ba} + \text{NO}_2$ .<sup>36</sup>

The  $\text{NO}_2$  beam was formed by passing a noble gas through liquid or solid  $\text{NO}_2$  cooled in a thermostatted temperature bath. The seeded molecular beams were typically 5-10%  $\text{NO}_2$  in He; the lowest collision energy was obtained using neat  $\text{NO}_2$  vapor. In each case, the  $\text{NO}_2$  beam nozzle was heated to 200-250°C to minimize the formation of  $\text{N}_2\text{O}_4$  and larger clusters. Mass scans with the detector looking directly into the molecular beam indicated that the concentration of such species were negligible. To be certain, parallel experiments were run using 100°C and 250°C nozzle temperatures in He carrier gas. The same beam velocity was attained in each experiment by addition of Ne to the He in the higher temperature experiment. The  $\text{BaO}$  product angular distributions were found to be the same, indicating negligible contribution from reaction of  $\text{N}_2\text{O}_4$ . If there was substantial contribution from reaction of  $\text{N}_2\text{O}_4$ , its higher concentration in

the lower temperature experiment should have led to an increase of product at larger scattering angles since the center-of-mass angle associated with Ba + N<sub>2</sub>O<sub>4</sub> scattering is substantially greater than that for Ba + NO<sub>2</sub>.<sup>37</sup>

For each species (Ba, BaO or BaNO), the data was recorded with the mass spectrometer tuned to the parent ion mass. The dominant (71%) <sup>138</sup>Ba isotope-containing species was monitored in each case. Product angular and velocity distributions were obtained by running parallel experiments at various detector angles with the laser on and off. In all cases, tuning the laser well away from the barium atomic resonance had the same effect as blocking the laser beam.

Angular distributions for Ba and BaO were obtained by modulating the NO<sub>2</sub> beam using a 150 Hz tuning tuning fork chopper. Time of flight spectra were obtained using the cross correlation method.<sup>38</sup> The BaNO angular distributions were obtained by integrating the area under the peak in the time of flight spectra obtained at appropriate detector angles.

### III. RESULTS AND ANALYSIS

#### A. Ba(<sup>1</sup>S) + NO<sub>2</sub> → BaO + NO

Product angular distributions and time-of-flight data were recorded with the mass spectrometer set at Ba<sup>+</sup> (m/e=138) and BaO<sup>+</sup> (m/e=154) for the above reaction at 4 collision energies in the range 5-59 kcal/mole. The angular distributions of BaO exhibited two distinct peaks; at all collision energies the peak near 0° was larger than the wide angle peak (Fig. 2). The observed signal was very strong; typically only 10 mins. of averaging was required at each angle for each time-of-flight spectrum. The Ba<sup>+</sup> data at all angles wider than 10° was very similar to the BaO data, indicating that the signal obtained for Ba<sup>+</sup> primarily results from fragmentation of BaO in the ionizer with a small contribution from nonreactive scattering. Our observations are consistent with a large reaction cross section and the previous conclusions of "reactions at every collision."<sup>13</sup>

In the analysis of the BaO data, an important concern is the internal energy dependence of the fragmentation pattern of BaO upon 200V electron impact ionization. This turned out to be an important factor for NaO in our recent study<sup>39</sup> of the reaction  $\text{Na} + \text{O}_3 \rightarrow \text{NaO} + \text{O}_2$ . In that case, the fragmentation ratio  $\text{Na}^+/\text{NaO}^+$  increased substantially with internal excitation of NaO, and we included the dependence in the analysis. We recorded the  $\text{Ba}^+$  and  $\text{BaO}^+$  time-of-flight data from  $\text{Ba} + \text{NO}_2$  at the center-of-mass angle, where products with the full range of internal energies contribute to the TOF spectrum. The shape of both spectra were identical, indicating that internal energy of the precursor BaO is not high enough in the present case to noticeably affect the fragmentation pattern. Similar conclusions have been made by others in the past.<sup>19,40</sup> It is important to note that our detector is not state specific; we have no way to unambiguously distinguish between different nascent electronic states of BaO unless their times of arrival are well separated. However, excited states are known to be a minor contribution to the total reaction cross section. They will radiate<sup>31</sup> during their flight to the ionizer ( $T > 100 \mu\text{sec}$ ), and will be detected with the same efficiency as nascent ground state products. Formation of electronically excited  $\text{NO}(\text{A}^2\Sigma^+)$  is not thermodynamically possible at the collision energies employed in this experiment.<sup>30</sup>

We now consider possible explanations for the observed product angular distribution. Most commonly, the characteristic forward-backward peaking observed here results from decay of long-lived collision intermediates. As was discussed by Miller, et. al.,<sup>24</sup> decay of a prolate complex with a lifetime greater than a few rotational periods ( $> 1\text{-}2\text{psec}$ ) is expected to lead to a forward-backward symmetric center-of-mass product angular distribution. The degree of peaking at the poles ( $\theta_{\text{CM}} = 0^\circ$  and  $180^\circ$ ) with respect to  $\theta_{\text{CM}} = 90^\circ$  provides information about the disposal of the total angular momentum into product rotation. Upon examining the laboratory angular distributions, one might anticipate that the CM angular distribution was completely forward-backward symmetric with the measured angular distribution distorted in favor of the forward peak due to the transformation Jacobian relating the product intensities in the laboratory to that in the center-of-mass coordinate system.<sup>24</sup>

$$I_L(\Theta, v) = I_{cm}(\theta, u) \frac{v^2}{u^2}$$

For decay of long-lived complexes, the recoil velocity in the center-of-mass frame of reference ( $u$ ) is independent of angle. However, as can be seen from the Newton diagram (Fig. 2), the laboratory center-of-mass angle is less than  $45^\circ$  in this experiment. As a consequence, at small lab angles the lab velocity ( $v$ ) associated with a given center-of-mass velocity ( $u$ ) is greatest in the forward direction, leading to enhancement of  $I_L(\Theta, v)$ .

We initially attempted to fit the time-of-flight and angular distributions using an iterative forward convolution method with a single uncoupled CM angular ( $T(\Theta)$ ) and translational energy ( $P(E)$ ) distribution. This approach is expected to be rigorously correct for a single channel involving decay of complexes with lifetimes of several rotational and many vibrational periods. An uncoupled  $T(\Theta)$  and  $P(E)$  is also likely to be a reasonable approximation if 'osculating'<sup>41-44</sup> complexes were involved with lifetimes on the order of one rotational period. Although the assumption of separability of the angular and energy distribution allowed us to reproduce the qualitative features of the product time-of-flight and angular distributions, it was not possible to obtain a fit commensurate with the quality of the raw data, which was reproducible and of good signal-to-noise ratio (Fig. 3).

Our data indicates that the average translational energy release in the forward direction is **smaller** than in the backward hemisphere. This leads us to conclude that the assumption of a single uncoupled  $T(\theta)$  and  $P(E)$  (i.e. a single mechanism involving complexes) is unsatisfactory. The existence of osculating complexes with relatively short lifetimes can be ruled out since it is known that product angular distributions from their decay will be rather sensitive to collision energy. If the complexes lived for  $\sim 1$  rotational period at low collision energy, upon increasing the collision energy we should observe substantially increased forward scattering as their statistical lifetimes decrease. Such a transition has been observed in other systems.<sup>41-44</sup> In the

### B. $\text{Ba}(^1\text{S}, ^1\text{P}) + \text{NO}_2 \rightarrow \text{BaO} + \text{NO}$

The BaO angular distributions shown in Fig. 10 show the effect of electronic excitation of the Ba atoms at the interaction region. The beam contained 30% Ba ( $^1\text{S}$ ), 35% ( $^1\text{P}$ ) and 35% ( $^1\text{D}$ ). Although the effect was rather small, the BaO intensity was found to increase at lab angles smaller than  $25^\circ$  and greater than  $50^\circ$ . The signal decreased slightly between  $25^\circ$  and  $50^\circ$ . The Newton diagram (Fig. 10) shows circles for the maximum BaO CM velocities from reaction of Ba( $^1\text{P}$ ) (solid) and Ba( $^1\text{S}$ ) (dotted). Based on the increased BaO signal observed near the edges of the Newton sphere, we conclude that electronic excitation of the incident Ba leads to formation of BaO with slightly greater average translational energy than reaction of the ground state atom. Because the signal increased the same amount in the forward and backward hemispheres, formation of ground state BaO from electronically excited Ba primarily results from decay of long-lived collision complexes, as in the ground state reaction. Excitation of the barium atoms upstream of the collision zone results in 60% Ba ( $^1\text{D}$ ), and 40%  $^1\text{S}$ . The BaO angular distribution from Ba ( $^1\text{D}$ ) was very similar; however, there was a smaller increase at wide lab angles since less energy was available from reaction of Ba( $^1\text{D}$ ) than Ba( $^1\text{P}$ ).

### C. $\text{Ba} + \text{NO}_2 \Rightarrow \text{BaNO} + \text{O}$

The occurrence of a chemically distinct second channel, BaNO + O was observed from Ba( $^1\text{S}$ ) + NO<sub>2</sub> at collision energies above 40 kcal/mole. The observed threshold collision energy from reaction of electronically excited Ba ( $^1\text{D}$ ) was below 25 kcal/mole. Unlike BaO, the energy dependence of the BaNO fragmentation pattern cannot be easily obtained. Although this species is considerably more weakly bound than BaO, ionization of this radical likely involves removal of a nonbonding electron. This suggests that the internal energy dependence of the BaNO fragmentation pattern is probably not a major concern. Indeed, the product time-of-flight for the NO<sup>+</sup> daughter ion from BaNO could be observed and appeared to be the same as BaNO<sup>+</sup>. From the observation of the NO<sup>+</sup> daughter ion, the location of the mass peak, and observation that the signal disappeared upon turning off the ionizer, we were able to rule out the possibilities that the signal resulted from BaO<sub>2</sub><sup>1,34a</sup> leakage through the mass spectrometer, electronically excited or

Rydberg Ba atoms<sup>46</sup>, or nascent ions.<sup>36</sup>

In the  $\text{Ba}(^1\text{S}) + \text{NO}_2$  reaction, the BaNO product intensity was found to be rather weak, increasing with increasing collision energy. Unlike the dominant  $\text{BaO} + \text{NO}$  channel, BaNO from reaction of ground state Ba was only observed over a narrow range of laboratory angles, peaking away from the relative velocity vector. (Fig. 11, filled circles). The  $\text{BaNO} + \text{O}$  channel from  $\text{Ba}(^1\text{S}) + \text{NO}_2$  appears to be completely independent of the  $\text{BaO} + \text{NO}$  channel. The BaNO time-of-flight spectra for reaction of  $\text{Ba}(^1\text{S})$  are shown in Fig. 12. The slower broad peak in the time of flight spectrum remained even when the electron bombardment ionizer was turned off. It results from surface ionization of barium atoms at the back wall of the detector. The product angular and time-of-flight distributions were fit using a single uncoupled  $T(\theta)$  and  $P(E)$ , (Fig. 14). The BaNO product flux contour map from reaction of ground state Ba is shown in Fig. 15.

At a collision energy of 59 kcal/mole, electronic excitation of the Ba atom to the  $^1,^3\text{D}$  states resulted in a twofold increase in BaNO signal, and a larger increase was seen from the  $^1\text{P}$  state. Unlike the ground state reaction, the best fit of the BaNO angular and velocity distribution from reaction of electronically excited  $\text{Ba}(^1\text{P}, ^1,^3\text{D})$  (Fig. 11- hollow squares, Fig. 13) resulted in a forward-backward symmetric center-of-mass angular distribution (Fig. 14). The angular distribution obtained by pumping the Ba atoms upstream of the collision zone to the metastable  $^1,^3\text{D}$  states was weaker, but qualitatively similar. The forward-backward symmetric angular distributions indicate that unlike the BaNO resulting from reaction of ground state  $\text{Ba}(^1\text{S})$ , formation of BaNO from excited state Ba primarily results from decay of long-lived collision complexes.

## IV. DISCUSSION

### A. $\text{Ba} + \text{NO}_2 \rightarrow \text{BaO} + \text{NO}$

#### i. Comparison to Past Work

Perhaps the most surprising result of our study is that the reaction  $\text{Ba} + \text{NO}_2 \rightarrow \text{BaO} + \text{NO}$  primarily involves long-lived collision complexes with large releases of translational energy. Since both of these primary conclusions disagree with those from the past work of others,<sup>18,19</sup> we first address this discrepancy. The most obvious difference between this experiment and previous work is the higher collision energy in the present work. The past experiments were conducted using a single mean collision energy of  $\sim 2\text{-}3$  kcal/mole whereas we studied the reaction at four energies with the lowest at 5 kcal/mole. An explanation for the discrepancy could be that a direct reaction mechanism with forward scattering occurs at the low collision energy of the previous work with the mechanism evolving into one with collision complexes at the higher energies employed here. This appears to be unlikely since the best fit to our data obtained at the lowest collision energy showed no enhancement of the forward scattering component. Moreover, such behavior would be exactly opposite of what is usually observed:<sup>41-44</sup> a decreased statistical lifetime of the complex is normally expected with increasing energy, leading to direct reaction at higher energy.

Another possible explanation for our result is that at higher collision energies, the divalent barium atom preferentially inserts into a covalent bond with formation of  $\text{O}^-\text{Ba}^{2+}\text{NO}^+$ . This would be somewhat analogous to the behavior we have recently observed in the reaction  $\text{Ba}(^1\text{D}) + \text{H}_2\text{O} \rightarrow \text{HBaOH}^* \rightarrow \text{BaOH} + \text{H}$ .<sup>47</sup> In such systems, a forward-backward angular distribution does not necessarily imply that the intermediates survive longer than one rotational period. Since insertion (or more likely, H-atom migration) could involve either of two identical O-H bonds, the symmetric BaOH angular distribution might simply reflect the  $\text{C}_{2v}$  symmetry of  $\text{H}_2\text{O}$ . Although it might seem that an analogous situation could exist here, we believe that such a situation is unlikely for two reasons. First, symmetry arguments indicate that insertion will be very unfavorable for  $\text{Ba}(^1\text{S}) + \text{NO}_2$ . More importantly, insertion of ground state  $\text{Ba}(^1\text{S})$  into  $\text{NO}_2$  is

likely to involve a large potential energy barrier since the process involves a nearly simultaneous transition from a covalent to a doubly ionic surface. This suggests that a potential energy barrier will exist in the entrance channel. There should be a negligible barrier in the exit channel, however, since decay of the vibrationally activated insertion intermediate to BaO + NO should only involve simple bond rupture. Thus, we expect that the products from an insertion mechanism should be vibrationally excited with small translational energy. This is not consistent with the low vibrational excitation measured in the LIF experiments<sup>17</sup> and large translational energy release that we observe. It appears that an OBaNO insertion intermediate does not play an important role in the reaction.

We believe that the conclusions based on the previous crossed beams experiments were incorrect. The danger of making conclusions based on angular distributions alone has been addressed previously.<sup>48</sup> Without velocity analysis, the transformation from the laboratory to center-of-mass angular distribution is not unique, especially when effusive beams are employed having broad velocity distributions. In particular, for a reaction of fast Ba atoms + slow NO<sub>2</sub> the transformation Jacobian will strongly enhance the forward peak, and the angular distribution alone will be rather insensitive to the actual T( $\theta$ ) P(E) combination. Since the metal-oxide bond energies decrease for the lighter alkaline earth atoms,<sup>30</sup> reactions of those species with NO<sub>2</sub> will be less exoergic. It is very likely that reaction of the other alkaline earths (Be is a possible exception) with NO<sub>2</sub> will also involve complex intermediates.<sup>49</sup>

## ii. Mechanism for Ba + NO<sub>2</sub> → BaO + NO

There is no question that this reaction is initiated by the well known "harpoon mechanism"<sup>2,3</sup> used to describe reactions such as K + Br<sub>2</sub> → KBr + Br. The energies of the lowest electronic states of NO<sub>2</sub><sup>-50</sup> are summarized in Table II together with the calculated ionic-covalent curve crossing radii and estimated reaction cross sections. The very large experimental reaction cross section can only be consistent with long range transfer into the half filled 6a<sub>1</sub> orbital (Fig. 16), corresponding to formation of ground state NO<sub>2</sub><sup>-</sup>(<sup>1</sup>A<sub>1</sub>)<sup>50</sup>. The analogy between the present reaction

and the alkali-halogen reaction extends no further, however. In the case of bromine, not only is the process  $\text{Br}_2 + e^- \rightarrow \text{Br}_2^- \rightarrow \text{Br} + \text{Br}^-$  exoergic,<sup>30</sup> but vertical electron attachment to  $\text{Br}_2$  results in formation of  $\text{Br}_2^-$  on the inner repulsive wall of the Br-Br interaction potential at an energy near the threshold for dissociation.<sup>6</sup> Electron attachment to  $\text{NO}_2$ , however, results in formation of a strongly bound anion; in fact  $D_0(\text{O}^--\text{NO})$  actually exceeds  $D_0(\text{O}-\text{NO})$ .<sup>22,30</sup> In low energy electron scattering, it is not surprising that the process  $\text{Br}_2 + e^- \rightarrow \text{Br}^- + \text{Br}$  is observed at electron energies down to 0 V.<sup>51</sup> The energy threshold for  $\text{NO}_2 + e^- \rightarrow \text{O}^- + \text{NO}$ , however, is equal to its endoergicity, 1.61eV.<sup>52</sup>

Although there is no information available as to the structure of gaseous  $\text{BaNO}_2$ , it was noted previously that considerable similarity is expected to the analogous alkali nitrites which are known to be stable molecules, even in the gas phase.<sup>53</sup> We have also noted that an  $\text{OBaNO}$  structure is unlikely. There appears to be no question that the alkali nitrites are ring shaped  $\text{C}_{2v}$  molecules with the metal cation symmetrically located in the plane of  $\text{NO}_2^-$ . This structure is supported by spectroscopic measurements both in matrix isolation experiments<sup>54</sup> and in the gas phase.<sup>55</sup> Ab initio calculations also indicate that a ring shaped structure is of lowest energy.<sup>56</sup> Experimental results on the alkaline earth nitrites<sup>57</sup> in rare gas matrices suggest the same structure or possibly a nonplanar structure with a poorly defined position of the  $\text{M}^+$  above the plane of the anion.

Orbital symmetry considerations (Fig. 16) indicate that interaction of  $\text{Ba}^+$  with  $\text{NO}_2^- 6a_1^2 (^1A_1)$  should be particularly favorable in the planar configuration in which the  $\text{Ba}^+$  lies on the  $\text{C}_{2v}$  axis between the two oxygen atoms. This will maximize the ionic attraction since the electron density on  $\text{NO}_2^-$  can be delocalized over the oxygen atoms and at the same time interact strongly with  $\text{Ba}^+$ . In addition, a net covalent interaction can be achieved by favorable overlap of the  $\text{Ba}^+(6s)$  orbital and the  $\text{NO}_2^- 6a_1$  orbital. Other planar geometries (such as  $\text{C}_s$ ) should be less stable due to poor orbital overlap. The two higher lying excited states of  $\text{NO}_2^-$  result from transfer of an electron into the unfilled  $2b_1$  orbital leading to the  $^1B_1$  and  $^3B_1$  states.<sup>50</sup> Not only does this orbital lie ~3eV higher than the  $6a_1$  (Table II), but based on orbital symmetry it appears that interaction of the excited states of  $\text{NO}_2^-$  with  $\text{Ba}^+$  will be weaker than for the ground state since overlap of

the orbitals lead to no net covalent attraction.

For nearly all trajectories, long range electron transfer into the  $6a_1$  orbital should be very favorable at  $r \approx 4.9 \text{ \AA}$ . Based on the geometries for  $\text{NO}_2$  and  $\text{NO}_2^-$  (Table III), and the O-O bonding character of the  $6a_1$  orbital, electron transfer will result in symmetric bending of  $\text{NO}_2^-$  with only a small amount of NO vibrational excitation.<sup>22</sup> We note that the asymmetric stretching mode (formally corresponding to the reaction coordinate) is not expected to be appreciably excited. Approach of Ba directly towards N along the  $C_{2v}$  axis is also expected to lead to efficient electron transfer but the resulting  $C_{2v}$   $\text{BaNO}_2$  molecule is probably less stable than the bidentate  $C_{2v}$  structure. However, such a species is still likely to survive for at least several vibrational periods since the departing  $\text{O}^-$  ion will be initially moving along one N-O bond axis. For a monodentate  $C_{2v}$   $\text{Ba}^+-\text{NO}_2^-$  molecule, this motion will oppose the  $\text{Ba}^+-\text{O}^-$  coulombic attraction, leading to a longer lifetime for decay of the ionic intermediate.

This reaction is very unusual since it is dominated by a mechanism involving collision complexes despite the fact that a very highly exoergic decay channel ( $\text{BaO} + \text{NO}$ ) is known to be accessed with a probability of nearly 100%. Since it is known that the slightly endoergic reaction  $\text{Cs} + \text{NO}_2 \rightarrow \text{CsO} + \text{NO}$  proceeds readily at a collision energy of 3 kcal/mole,<sup>25</sup> the potential energy barrier for decay of  $\text{Cs}^+\text{NO}_2^-$  to products must be nearly zero. If the barrier for decay of  $\text{Ba}^+\text{NO}_2^-$  to  $\text{Ba}^{2+}\text{O}^{2-} + \text{NO}$  was also negligible, survival of long-lived complexes for  $\tau \geq 1 \text{ psec}$  would require a Ba- $\text{NO}_2$  binding energy of  $>250 \text{ kcal/mole}$ .<sup>58</sup> This is far larger than is reasonable. We attribute the existence of complexes and the large amount of product translational energy from their decay to a large exit potential energy barrier for formation of products. This barrier in the exit channel appears to be a consequence of the divalent character of Ba. Decay of the complex to ground state molecules requires a substantial rearrangement of electronic structure, corresponding to transfer of the second valence electron necessary for formation of  $\text{Ba}^{2+}\text{O}^{2-}$ . The large exit barrier for decay of the complex apparently results from several factors. One factor is related to the most stable geometry for  $\text{Ba}^+\text{NO}_2^-$  likely being planar. Although the  $\text{NO}_2^-$  energy levels will be shifted significantly by the presence of  $\text{Ba}^+$ , it appears that the electronic rearrangement necessary for decay to products requires transfer of electron density into the  $2b_1$

lowest unoccupied molecular orbital of  $\text{NO}_2^-$ . As can be seen from Fig. 14, this is forbidden by orbital symmetry constraints for planar  $\text{Ba}^+\text{NO}_2^-$  complexes.

The height of the exit barrier for electronic rearrangement can be estimated from this work. It must lie below the energy of the reactants since we know that most complexes decay to products rather than back to reactants. Simple RRKM calculations<sup>58</sup> using  $D_0(\text{Ba-NO}_2)=65$  kcal/mole and reasonable estimates of  $\text{BaNO}_2$  vibrational frequencies suggest that at collision energies above 30 kcal/mole, complex lifetimes of  $\geq 1$  psec will result only if the barrier for decay of  $\text{BaNO}_2$  is greater than  $\sim 45$  kcal/mole. Using a 65 kcal/mole well depth, this implies that the barrier is not lower than 20 kcal/mole below the energy of separated  $\text{Ba} + \text{NO}_2$ . Based on our observation that the observed  $\text{Ba}^+$  signal primarily results from fragmentation of  $\text{BaO}$  in the ionizer, (rather than from decay of  $\text{BaNO}_2$  back to  $\text{Ba} + \text{NO}_2$ ), we believe that our lower limit of 45 kcal/mole is likely to be close to the true value. If the barrier were much nearer to the energy of separated  $\text{Ba} + \text{NO}_2$ , nonreactive scattering from decay of  $\text{BaNO}_2$  back to reactants should lead to an additional component in the  $\text{Ba}$  time-of-flight spectrum with relatively low translational energy release. Figure 17 shows the energy levels of all relevant chemical species involving ground state  $\text{Ba}$ -- solid lines denote reaction pathways.

## B. Source of the Forward Scattered $\text{BaO}$ Channel

Our experimental data indicates the existence of a second reaction channel leading to forward scattered  $\text{BaO}$  with smaller translational energy release than from the dominant channel. This channel results from a direct reaction mechanism; based on the observed product translational energy distribution, by conservation of energy the reaction exoergicity must be primarily channeled into product internal excitation. It might seem plausible that this direct reaction channel corresponds to formation of electronically excited  $\text{BaO}$ , best described as  $\text{Ba}^+\text{O}^-$ .<sup>31,59</sup> This explanation would appear to be particularly appealing since second electron transfer is not required for this product. However, our measurements indicate that the forward scattered channel represents  $20\pm 5\%$  of the total reaction cross section whereas the single collision chemiluminescence yield is known to be less than 0.2%.<sup>16,17</sup> Since there is no reason to believe

that electronically excited products should be preferentially formed in dark states, assuming that the chemiluminescence yield is correct, a large fraction of the forward scattered BaO products must be vibrationally excited ground state molecules.

Since a direct reaction mechanism implies a short lifetime for the ionic intermediate, it might seem at first surprising that the direct reaction mechanism is relatively minor. This indicates that the forward scattered BaO does not result from kinetic competition with the dominant channel involving collision complexes. Instead, the relatively small yield of direct, forward scattered products must reflect a small probability for avoiding the deep  $\text{Ba}^+\text{NO}_2^-$  well. There are two possible mechanisms whereby this may be achieved. Some trajectories can remain on the covalent surface by avoiding electron transfer at the first crossing. In this case, electron transfer at the second crossing is nearly certain and the reaction intermediate can be considered to be an excited state of  $\text{Ba}^+\text{NO}_2^-$  which will have a shorter lifetime due to its weaker bond. This mechanism appears to be dominant in the reaction  $\text{Li} + \text{NO}_2 \rightarrow \text{LiO} + \text{NO}$ , which was found to be direct without the involvement of long-lived collision complexes.<sup>28,29</sup> This model appears unlikely in the present case, however, since the relative yield of forward scattered products is not very sensitive to collision energy. Since adiabatic behavior at the outer crossing is expected to decrease with increasing collision energies,<sup>60</sup> if this explanation were correct we should have observed a substantial increase of forward scattering with increasing collision energy. Moreover, correlations<sup>61</sup> between curve crossing distance and electron transfer probability in atom-atom and atom-diatom systems indicate that at 4.9 Å, the electron transfer probability will be nearly 100%. The alternative explanation is that the direct reaction results from electron transfer into the  $6a_1$  orbital from Ba- $\text{NO}_2$  geometries which are unfavorable for formation of long-lived complexes. This situation would be expected to occur in those collisions where the  $\text{Ba}^+$  can approach very close to one oxygen atom in  $\text{NO}_2^-$ . In this case, a very close  $\text{Ba}^+\text{-O}$  interaction would be favorable for second electron transfer and formation of ground state products. Good coupling between the incident kinetic energy and the reaction coordinate facilitates second electron transfer and formation of vibrationally hot, forward scattered BaO.

## C. Ba + NO<sub>2</sub> → BaNO + O

### i) The Ba(<sup>1</sup>S) Reaction Mechanism

A number of observations allow us to gain considerable insight into the dynamics of this channel. The angular distribution from reaction of ground state Ba(<sup>1</sup>S) was found to peak over a very narrow range, well away from the relative velocity vector. Formation of BaNO results from a direct reaction, unlike the dominant ground state BaO channel. The small cross section and a narrow angular distribution indicates that successful reaction results from a very restricted range of collision geometries.

In the next section, we will argue that BaNO is best represented as Ba<sup>+</sup>NO<sup>-</sup>. An obvious question is whether long range electron transfer into the 6a<sub>1</sub> orbital of NO<sub>2</sub> precedes formation of BaNO + O. We believe that it does not; rather, BaNO likely results from trajectories which are able to avoid harpooning at the outer crossing point. The probability density maps for electrons in the 6a<sub>1</sub> and 2b<sub>1</sub> orbitals (Fig. 16) are useful in determining favorable and unfavorable molecular orientations for electron transfer. Although the shapes of the orbitals will become distorted upon close approach of Ba, they should be reasonable approximations outside the first ionic-covalent curve crossing radius (4.9Å). Transfer of an electron from the spherically symmetric Ba 6s orbital into the NO<sub>2</sub> 6a<sub>1</sub> orbital can be best avoided by approach of Ba towards N just off the C<sub>2v</sub> axis. This approach geometry will also lead to asymmetric stretching of NO<sub>2</sub>, an important requisite for reaction. The substantial threshold and narrow product angular spread is consistent with a narrow approach geometry and a need to couple translational energy into the asymmetric stretching of NO<sub>2</sub>. However, maintaining proper collision geometry alone is not likely to be sufficient to promote this reaction. Since electron transfer into the 6a<sub>1</sub> orbital leads to symmetric bending or symmetric stretching, only by remaining on the covalent surface at the outer crossing is it possible to excite the asymmetric NO<sub>2</sub> motion. The small product yield (<2% that of BaO) is consistent with a very small probability for avoiding electron transfer at the first ionic-covalent crossing.

Based on the translational energy measurements, we calculate  $D_0(\text{Ba-NO}) > 65$  kcal/mole (Section iii). Since  $D_0(\text{O-NO}) = 72$  kcal/mole<sup>30</sup>, the reaction is only slightly endoergic. However, the energy threshold for this reaction from  $\text{Ba}(^1\text{S})$  appears to be much greater than the endoergicity. It appears that the threshold is primarily due to a dynamic rather than thermodynamic requirement. The dynamic requirement is probably the need for nonadiabatic behavior at the outer crossing point and good coupling of the incident kinetic energy into the reaction coordinate, i.e. asymmetric N-O stretching. This is supported by our observation that the reaction is strongly promoted by very high collision energy. The probability of long range electron transfer depends on several factors.<sup>60,61</sup> These include the difference in the gradients for each potential energy surface in the vicinity of the crossing region, impact parameter, orientation of the  $\text{NO}_2$  molecule, radial velocity, and coupling matrix element. For the reaction of ground state  $\text{Ba}(^1\text{S})$ , formation of  $\text{BaNO}$  requires small impact parameter collisions. For small impact parameters, the relative velocity is almost entirely radial and an increase in collision energy can lead to substantially decreased adiabatic behavior and asymmetric motion of the  $\text{NO}_2$  molecule. This should lead to enhancement of  $\text{BaNO}$  by decreasing the probability for outer harpooning and permitting good coupling of the incident kinetic energy into the reaction coordinate.

## ii) The Effect of Electronic Excitation

Electronic excitation to the  $^1\text{P}$  state increases the first ionic-covalent curve crossing radius to  $\sim 15$  Å, leading to a substantially decreased probability for electron transfer into the  $6a_1$  orbital.<sup>61</sup> The next crossings correspond to transfer of the Ba 6s electron into the  $6a_1$  orbital (retaining the Ba 6p core) or transfer of the 6p electron into the  $2b_1$  orbital. Both processes correspond to formation of excited state  $\text{Ba}^+\text{NO}_2^-$ . Based on the  $\text{BaO}$  angular distributions, a large fraction of these excited complexes still survive for longer than one rotational period. At least part of this increased energy appears in relative translational motion of the recoiling  $\text{BaO/NO}$  products.

With electronic excitation to the  $1,3D$  states, we observed an approximately twofold enhancement of formation of  $BaNO + O$ . The yield was larger from the ( $1P$ ) state with an enhancement by a factor of 3-4. However, the products appear to result from decay long-lived complexes, whereas the reaction is direct from the ground state. This unusual behavior likely results from a substantial increase in the energy of the  $Ba^+NO_2^-$  complex due to electronic excitation of the incident Ba atom. In the case of ground state  $Ba(1S)$ , only a very small fraction of collisions could avoid the first electron transfer. With proper collision geometry and good coupling of incident collision energy into the reaction coordinate,  $BaNO + O$  resulted from a direct reaction mechanism. In the reaction of electronically excited Ba, decay of internally excited  $Ba^+NO_2^-$  complexes leads to the formation of  $BaNO + O$  products in addition to the dominant  $BaO + NO$ .

### iii) The Dissociation Energy of BaNO

The Ba-NO binding energy may be derived from the translational energy distribution for  $Ba(1S) + NO_2 \rightarrow BaNO + O$ . The following expression relating the energy of the reactants to that of the products is based on conservation of energy:

$$E_{\text{coll}} + E_{\text{int},NO_2} - D_o(O-NO_2) = E_{\text{int},BaNO} + E_{\text{int},O} + E_{\text{trans},BaNO/O} - D_o(Ba-NO). \quad (2)$$

By assuming efficient cooling of rotational but not vibrational energy of  $NO_2$  in the supersonic expansion,  $E_{\text{int},NO_2} \approx 2$  kcal/mole. The following equation, derived from (2) is actually an equality if the fastest BaNO products correspond to formation of BaNO in its ground rovibrational states and the oxygen atom is  $O(3P)$ :

$$D_o(Ba-NO) \geq E_{\text{trans},BaNO/O} + D_o(O-NO_2) - E_{\text{coll}} - E_{\text{int},NO} \quad (3)$$

Using  $E_{\text{coll}} = 60$  kcal/mole and  $D_o(O-NO_2) = 72$  kcal/mole, we calculate  $D_o(Ba-NO) \geq 65$  kcal/mole,

with the uncertainty not greater than 20 kcal/mole. Uncertainties arise in fitting the translational energy distribution and from the spread of the velocity distribution of the Ba beam. Since it is likely that at least some ground state products are formed in the reaction, we conclude that  $D_0(\text{Ba-NO}) = 65 \pm 20$  kcal/mole.

There has been no previous direct observation of BaNO in the gas phase. In fact, as far as we know, this is the first direct observation of an isolated gaseous metal mononitroxide. However, infrared spectra of alkali<sup>62</sup> and alkaline earth<sup>57</sup> nitroxides have been recorded under matrix isolation conditions. Based on that work, it was concluded that the molecules are ionic: isotope shifts in the IR spectra suggested a bent or linear  $M^+NO^-$  molecule (rather than  $M^+ON^-$ ) in all cases except  $Li^+ON^-$ . Although no binding energies are available for other nitroxides, it is interesting to compare BaNO to known metal-dioxygen compounds. As perhaps one might expect,  $D_0(\text{Ba-NO})$  is comparable to singly ionic metal superoxides rather than the alkaline earth-dioxygen molecule which appears to have substantial doubly ionic character:  $D_0(\text{Na-O}_2) = 48.2$  kcal/mole<sup>63</sup>,  $D_0(\text{Ba-O}_2) = 120 \pm 20$  kcal/mole<sup>1,34</sup>.

#### D. The Absence of $\text{Ba} + \text{NO}_2 \rightarrow \text{BaO}_2 + \text{N}$

Considerable effort was devoted to observing this reaction since there was good reason to believe that it might occur. Electron transfer into the  $6a_1$  orbital strongly enhances bonding between the oxygen atoms with the O-N-O bond angle decreasing from  $134.1^\circ$  to  $115.4^\circ$  (Table III). The reaction  $B + \text{NO}_2 \rightarrow \text{BO}_2 + \text{N}$  has been observed by Green and Gole<sup>64</sup> and was attributed to rapid scissoring of the  $\text{NO}_2^-$  molecule after electron transfer. Other triatomic oxidants such as  $\text{O}_3$  and  $\text{ClO}_2$  did not lead to formation of  $\text{BO}_2$  since the bond angles in those molecules are not appreciably different from their anions. Dissociative electron attachment to  $\text{NO}_2$  is known to lead

to formation of  $O^-$ ,  $NO^-$  and  $O_2^-$  at 1.61 eV, 3.11 eV, and 4.03 eV, respectively.<sup>52</sup> Since these energies are the thermodynamic thresholds for the processes,<sup>30,52</sup> we postulated that with electronic excitation or at high collision energy, nascent  $BaO_2$  might be formed from reaction of  $Ba + NO_2$ .

The  $BaO_2 + N$  channel either does not occur at all, or is below the sensitivity of the experiment. There was no evidence that electronic excitation promotes this channel. The cross section must be below  $1\text{\AA}^2$  for formation of  $BaO_2 + N$ . It appears that the contrasting behavior between B and Ba arises primarily due to the ionization potential of B ( $8.3\text{eV}$ )<sup>21</sup> being considerably higher than that of Ba ( $5.2\text{eV}$ )<sup>21</sup>. In the case of Ba, electron transfer occurs at long range ( $\sim 4.9\text{\AA}$ ) whereas much closer distance is required for B ( $\sim 2.4\text{\AA}$ ). This difference appears to be critically important to the outcome of the chemical reaction. In the case of B, electron transfer and symmetric bending of  $NO_2$  will only occur when the B atom is essentially within the attractive well of the very strongly bound B- $O_2$  interaction potential. In the case of Ba, however, the ionic complex will execute many vibrations before the  $Ba^+$  can approach within the close range required for formation of  $BaO_2$ . Intramolecular energy redistribution within the complex leads to randomization of the initial symmetric bending motion. This results in long-lived complexes which decay to  $BaO + NO$ -- apparently the potential energy barrier for formation of  $BaO_2 + N$  is large. In those collisions where electron transfer into the  $6a_1$  orbital can be avoided, the dominant chemical product is  $BaNO + O$  rather than  $BaO_2 + N$ .

## V. CONCLUSIONS

We have found the chemistry of the  $Ba + NO_2$  reaction to be substantially more complex than previously believed. Our results on  $Ba + NO_2$  disagree with the earlier conclusions,<sup>18,19</sup> which were based solely on product angular distributions. We conclude that long-lived  $Ba^+NO_2^-$  intermediates are involved in the majority of all reactive trajectories despite reaction exoergicities that are comparable to complex well depths. This rather unusual behavior appears to be a

dynamic consequence of the divalent nature of barium: decay of the initially formed complex to ground state molecules involves a substantial potential energy barrier. This barrier is associated with the electronic rearrangement necessary for the initially formed singly ionic  $\text{Ba}^+\text{NO}_2^-$  complex to decay to ground state doubly ionic  $\text{Ba}^{2+}\text{O}^{2-} + \text{NO}$ . A very large release of translational energy, the magnitude of which is perhaps unprecedented from decay of collision complexes, results from a barrier to second electron transfer followed by strong repulsion of the stable  $\text{BaO} + \text{NO}$  products.

Two additional direct reaction channels were observed. A minor  $\text{BaO} + \text{NO}$  channel led to forward scattering of the metal oxide with a relatively small release of translational energy. Our observation that the yield of forward scattered products is larger than the known chemiluminescent yield indicates that this channel corresponds primarily to formation of vibrationally hot ground state  $\text{BaO}$  from direct reaction involving small impact parameter collisions. A previously unknown molecule,  $\text{BaNO}$ , was observed as a nascent minor product from  $\text{Ba} + \text{NO}_2$ . Unlike the dominant  $\text{BaO}$  channels that involve outer harpooning, formation of  $\text{BaNO}$  from  $\text{Ba}(^1\text{S})$  likely results from the small fraction of collision geometries that avoid long range electron transfer.

Even with electronic excitation of the incident barium atom, reactions involving long-lived collision complexes continued to dominate the neutral product channels.<sup>46</sup> Electronic excitation results in increased internal excitation of the  $\text{Ba}^+\text{NO}_2^-$ , leading to a larger average translational energy release in the  $\text{BaO} + \text{NO}$  products. Whereas complexes resulting from collisions of ground state  $\text{Ba}$  only decayed to  $\text{BaO} + \text{NO}$ , a small fraction of those from electronically excited  $\text{Ba}$  also decayed to  $\text{BaNO} + \text{O}$ .

## VI. ACKNOWLEDGEMENTS

The authors thank Dr. M.H. Covinsky for discussions relating to the dynamics of electron transfer reactions. HFD acknowledges NSERC (Canada) for a 1967 Science and Engineering Fellowship, and AGS thanks the NSF for a Graduate Fellowship. This work was supported by the Director, Office of Energy Research, Office of Basic Energy Sciences, Chemical Sciences Division of the U.S. Department of Energy under Contract No. DE-AC03-76SF00098.

## VII. REFERENCES

1. A brief account of some this work was presented previously: *Ber. Bunsenges. Phys. Chem.* 94, 1193, (1990).
2. a) M. Polanyi, *Atomic Reactions* (Williams and Norgate, Ltd.), London (1932). b) M.G. Evans and M. Polanyi, *Trans. Faraday Soc.*, 35, 178 (1939).
3. D.R. Herschbach, *Appl. Opt. Supp.* 2, 128 (1965).
4. J.L. Magee, *J. Chem. Phys.*, 8, 687, (1940).
5. R.D. Levine, R.B. Bernstein, "*Molecular Reaction Dynamics and Chemical Reactivity*", Oxford University Press, New York, (1987).
6. R.R. Herm in "*Alkali Halide Vapors*", P. Davidovits, D.L McFadden, Academic Press, New York, 1979.
7. a) S. Datz and R.E. Minturn, *J. Chem. Phys.*, 41, 1153, (1964). b) R.E. Minturn, S. Datz, R.L. Becker, *J. Chem. Phys.*, 44(3), 1149, (1966). c) K.R. Wilson, G.H. Kwei, J.A. Norris, R.R. Herm, J.H. Birely, and D.R. Herschbach, *J. Chem. Phys.*, 41, 1154, (1964). d) J. H. Birely, R.R. Herm, K.R. Wilson, D.R. Herschbach, *J. Chem. Phys.*, 47(3),993, (1967).

8. a) D.R. Herschbach, G.H. Kwei, J.A. Norris, *J. Chem. Phys.*, **34**, 1842, (1961). b) D.R. Herschbach, *Disc. Faraday Soc.*, **33**, 149, 281 (1962).
9. a) E.H. Taylor and S. Datz, *J. Chem. Phys.*, **23**, 1711 (1955); **25**, 389, 395 (1956). b) T.R. Touw and J.W. Trischka, *J. Appl. Phys.*, **34**, 3635 (1963).
10. Y.T. Lee, J.D. MacDonald, P.R. LeBreton, and D.R. Herschbach, *Rev. Sci. Instrum.*, **40**, 1402 (1969).
11. a) A. Schultz, H.W. Cruse and R.N. Zare, *J. Chem. Phys.*, **57**(3) 1354 (1972). b) H.W. Cruse, P.J. Dagdigian, R.N. Zare, *Faraday Disc. Chem. Soc.*, **55**, 277 (1973). c) R.N. Zare, P.J. Dagdigian, *Science*, **185**(4153), 739 (1974).
12. a) C.D. Jonah, R.N. Zare, and Ch. Ottinger, *J. Chem. Phys.* **56**, 263, (1972). b) K.G. Anlauf, P.E. Charters, D.S. Horne, R.G. Macdonald, D.H. Maylotte, J. C. Polanyi, W.J. Skrlac, D.C Tardy, and K.B. Woodall, *J. Chem. Phys.*, **53**, 4091 (1970) and references therein.
13. Ch. Ottinger and R.N. Zare, *Chem. Phys. Lett.*, **5**, 243 (1970).
14. A. Schultz and R.N. Zare, *J. Chem Phys.* **60**, 5120 (1974).
15. C.R. Dickson, S.M. George, and R.N. Zare, *J. Chem. Phys.* **67**, 1024 (1977).
16. For a complete list of papers up to 1982, see J.J. Reuther and H.B. Palmer, *J. Chem. Phys.* **77**(1), 83 (1982).
17. Y.C. Hsu and J.G. Pruett, *J. Chem. Phys.* **76**(12), 5849 (1981).
18. J.A. Haberman, K.G. Anlauf, R.B. Bernstein, F.J. Van Itallie, *Chem. Phys. Lett.*, **16**(3), 442 (1972).
19. R.R. Herm, S.M. Lin, C.A. Mims, *J. Phys. Chem.* **77**(25), 2931, 1973.
20. J.H. Birely and D.R. Herschbach, *J. Chem. Phys.*, **44**(4) 1690 (1966).
21. R.C. Weast, Ed., *CRC Handbook of Chemistry and Physics*, CRC Press, Inc. Boca Raton, Fla. (1987).
22. K.M. Ervin, J. Ho, and W.C. Lineberger, *J. Phys. Chem.*, **92**, 5405, (1988).

23. a) D.O. Ham, J.L. Kinsey and F.S. Klein, *Disc. Faraday. Soc.* 44, 174 (1967). b) D.O. Ham, J.L. Kinsey, *J. Chem. Phys.*, 48(2), 939 (1968). c) D.O. Ham and J.L. Kinsey, *J. Chem. Phys.*, 53(1), 285 (1970).
24. a) W. B. Miller, S.A. Safron, D.R. Herschbach, *Disc. Faraday Soc.*, 44, 108, (1967). b) W. B. Miller, Thesis, Harvard University, 1969.
25. R.R. Herm and D.R. Herschbach, *J. Chem. Phys.* 52(11), 5783 (1970).
26. The reaction  $\text{Cs} + \text{CH}_3\text{NO}_2 \rightarrow \text{CsNO}_2 + \text{CH}_3$  is known to be exothermic (Ref. 25). Thus  $D_0(\text{Cs-NO}_2) > 60$  kcal/mole. Based on an empirical correlation between bond energy and electron affinities (Ref. 25), we calculate  $D_0(\text{Cs-NO}_2) = D_0(\text{CsO}) + \text{EA}(\text{NO}_2) - \text{EA}(\text{O}) = 89$  kcal/mole. However, this estimate is almost certainly too high since it neglects the different interionic distances for  $\text{Cs}^+\text{-O}^-$  and  $\text{Cs}^+\text{-NO}_2^-$ .
27. H.F. Davis, A.G. Suits, Y.T. Lee, to be published.
28. The reaction  $\text{Li} + \text{NO}_2$  appears to be anomalous since velocity and angular analysis has indicated that the reaction is direct with preferential forward scattering of the LiO product. It has been argued that the  $\text{Li}^+\text{NO}_2^-$  intermediate is formed in an electronically excited state which is too weakly bound to survive even one rotational period. See Ref. 29.
29. a) C.M. Sholeen and R.R. Herm, *J. Chem. Phys.*, 64(12), 5261, (1976). b) D.D. Parrish and R.R. Herm, *J. Chem. Phys.*, 54(6), 2518 (1971).
30. a) JANAF Thermochemical Tables, 3rd ed. *J. Physical and Chemical Ref. Data.*, Volume 14, (1985) Supplement No.1. (b) *J. Phys. Chem. Ref. Data* 12(4) 982 (1983).
31. J.G. Pruett and R.N. Zare, *J. Chem. Phys.*, 62, 2050 (1975).
32. It has generally been assumed that potential energy barriers to decay of the complex would be small.
33. C.E. Moore, *Atomic Energy Levels*, National Stand. Ref. Data Ser. (National Bureau of Standards, Washington D.C, 1971)
34. a) H. F. Davis, A.G. Suits, and Y.T. Lee, to be submitted to *J. Chem. Phys.* b) H.F. Davis, A.G. Suits, M.H. Covinsky, and Y.T. Lee, to be submitted to *Rev. Sci. Instrum.*
35. S. Niggle, M.C.E. Huber, *Phys. Rev. A.*, 35(7), 2908, (1987).

36. The formation of nascent ions is discussed in a separate article. A polarization effect was observed in the ion channels. A.G. Suits, H. Hou, H.F. Davis, and Y.T. Lee, *J. Chem. Phys.*, accepted for publication.
37. The reactivity of  $\text{Ba} + \text{N}_2\text{O}_4$  has been investigated. See: D.J. Wren, and M. Menzinger, *Chem. Phys.*, 66, 85 (1982).
38. G. Comsa, R. David, B.J. Schumacher, *Rev. Sci. Instrum.*, 52(6), 789 (1981).
39. M.H. Covinsky, A.G. Suits, H.F. Davis, and Y.T. Lee, *J. Chem. Phys.*, submitted for publication.
40. C. Batalli-Cosmovici and K.W. Michel, *Chem. Phys. Lett*, 11, 245 (1971).
41. Y.T. Lee, J.D. McDonald, P.R. LeBreton and D.R. Herschbach, *J. Chem. Phys.*, 49, 2447, (1968).
42. C. H. Becker, P. Casavecchia, P.W. Tiedmann, J.J. Valentini, and Y.T. Lee, *J. Chem. Phys.*, 73(6), 2833 (1980).
43. R. Wolfgang, *Acc. Chem. Res.*, 3, 48, (1969).
44. G.A. Fisk, J.D. McDonald, D.R. Herschbach, *Disc. Faraday. Soc.*, 44, 228 (1967).
45. a) T. P. Parr, A. Freedman, R. Behrens, Jr., and R.R. Herm, *J. Chem. Phys.*, 67(5), 2181, (1977); b) S.-M. Lin, C.A. Mims, and R.R. Herm, *J. Phys. Chem.*, 77(5), 569 (1973).
46. We have observed formation of Rydberg sodium atoms in recent experiments. These are formed in the ionizer and subsequently undergo surface ionization at the back surface of the detector. This signal can be easily distinguished from product molecules: The peak is much slower than the reactive signal, it is independent of mass setting, and disappeared upon turning off the ionizer.
47. H.F. Davis, A.G. Suits, Y.T. Lee, C. Alcaraz and J.M. Mestdagh, *J. Chem. Phys.*, to be submitted for publication, and references therein.
48. J.M. Farrar, and Y.T. Lee, *Ann. Rev. Phys. Chem.*, 25, 357, (1974).
49. We found that the reaction  $\text{Mg} + \text{NO}_2 \rightarrow \text{MgO} + \text{NO}$  also involves long-lived collision complexes (work in progress).

50. The energies of the excited states of  $\text{NO}_2^-$  are based on the average of several experimental values. See P.A. Benioff, *J. Chem. Phys.*, 68(8), 3405 (1978) and references therein.
51. D.C. Frost, C.A. McDowell, *Can. J. Chem.*, 38, 407 (1960).
52. R. Aboual, R. Paineau and F. Fiquet-Fayard, *J. Phys. B.*, 9(2), 303, (1976).
53. a) C.J. Hardy, B.O Field, *J. Chem. Soc.*, 5130, (1963).  
b) A. Büchler and J.L. Stauffer, *J. Phys. Chem.* 70(12), 4092, (1966).
54. M. Barbeschi, L. Bencivenni, F. Ramondo, *Chem. Phys.*, 112, 387, (1987).
55. a) E.N. Verkhouturov, A.V. Makarov and O.T. Nikitin, *Vestn. Mosk. Univ. Khim.* 17, 299, (1976). b) A.M. Shapovalov, V.F. Shevelkov and A.A. Maltsev, *Vestn. Mosk. Univ. Khim.* 14, 151, (1973).
56. F. Ramondo, *Chem. Phys. Lett.*, 156(4), 346 (1989).
57. a) D.E. Tevault and L. Andrews, *Chem. Phys. Lett.*, 48(1), 103 (1977). b) D.E. Tevault and L. Andrews *J. Phys. Chem.* 77(13), 1640, (1973).
58. The original version of the RRKM program employed in estimating complex lifetimes was written by W.L. Hase and D.L. Bunker; See P.J. Robinson and D.A. Holbrook, Unimolecular Reactions, Wiley-Interscience, New York, 1972.
59. S.R. Langhoff, C.W. Bauschlicher, Jr., H. Partridge, *J. Chem. Phys.*, 84(8) 4474 (1986).
60. N.F. Mott, H.S.W. Massey, *The Theory of Atomic Collisions*, 3rd ed. (Oxford University Press, London, 1965).
61. R.E. Olson, F.T. Smith and E. Bauer, *Appl. Optics*, 10, 1848 (1971).
62. a) D. E. Tevault and L. Andrews, *J. Phys. Chem.*, 77(13), 1646 (1973). b) W. L. Andrews, G.C. Pimentel, *J. Phys. Chem.*, 44(6), 2361, (1966).
63. J.M.C. Plane, B. Rajasekhar, L. Bartolotti, *J. Phys. Chem.* 93, 3141 (1989).
64. G. J. Green and J. L. Gole, *Chem. Phys. Lett*, 69(1), 45, (1980).
65. G. Herzberg, *Spectra of Diatomic Molecules*, Van Nostrand, Princeton, N.J. (1950).

TABLE I. Thermodynamics of Possible Ba(<sup>1</sup>S) + NO<sub>2</sub> Reactions

Reaction	$\Delta H$ (kcal/mole)	Ref
BaO(X <sup>1</sup> $\Sigma^+$ ) + NO	-61	30
BaO(A <sup>1</sup> $\Sigma^+$ ) + NO	-11	30
BaO(A <sup>1</sup> $\Pi$ ,a <sup>3</sup> $\Pi$ ) + NO	-11	30
BaNO + O	+7	1, This Work
BaO <sub>2</sub> + N	-12	1, 34a

TABLE II. States of NO<sub>2</sub><sup>-</sup>

State	E(eV) <sup>a</sup>	R <sub>x</sub> (Å) <sup>b</sup>	$\sigma_{\text{calc}}$ (Å <sup>2</sup> ) <sup>c</sup>
<sup>1</sup> A <sub>1</sub> ....6a <sub>1</sub> <sup>2</sup>	-2.27 <sup>d</sup>	4.9	75
<sup>3</sup> B <sub>1</sub> ....6a <sub>1</sub> <sup>1</sup> ,2b <sub>1</sub> <sup>1</sup>	+0.57 <sup>e</sup>	2.5	20
<sup>1</sup> B <sub>1</sub> ....6a <sub>1</sub> <sup>1</sup> ,2b <sub>1</sub> <sup>1</sup>	+1.23 <sup>e</sup>	2.2	15

a. Energy relative to NO<sub>2</sub> +  $\epsilon$ .

b. Ionic covalent curve crossing radius calculated using  $R_x(\text{\AA}) = 14.4/(\text{I.P.}_{\text{Ba}} - E)(\text{eV})$ .

c. Estimated harpooning cross section based on  $\sigma_{\text{calc}} = \pi R_x^2$

d. Electron affinity of NO<sub>2</sub> from Ref 22.

e. Energies relative to NO<sub>2</sub> +  $\epsilon$  based on NO<sub>2</sub> electron affinity and excited state energies tabulated in Ref 50.

TABLE III: Molecular Parameters

Species	$R_{N-O}(\text{\AA})$	$\alpha$ (degrees)
$\text{NO}_2(X^2A_1)$	1.19389(4) <sup>a</sup>	133.857(3) <sup>a</sup>
$\text{NO}_2(X^1A_1)$	1.25(2) <sup>a</sup>	$117.5 \pm 2$ <sup>a</sup>
$\text{NO}(X^2\Pi)$	1.1508 <sup>b</sup>	-

a. Ref 22, and references therein. b. Ref 65

### VIII. FIGURE CAPTIONS

1. Top view of the crossed molecular beams apparatus.
2. BaO laboratory angular distribution for  $\text{Ba} + \text{NO}_2 \rightarrow \text{BaO} + \text{NO}$  at collision energy of 12.5 kcal/mole.  $\circ$  Experimental points. — Total fit to data.  $\cdots$  Contribution from channel 1.  $----$  Contribution from channel 2. The nominal Newton diagram is shown with a limiting circle indicating the maximum center-of-mass velocity for BaO based on the known reaction exoergicity for formation of ground state products.
3. BaO product time-of-flight spectra at indicated laboratory angles for  $\text{Ba} + \text{NO}_2 \rightarrow \text{BaO} + \text{NO}$  at collision energy of 12.5 kcal/mole.  $\circ$  Experimental data. — Total fit to data.  $\cdots$  Contribution from channel 1.  $-----$  Contribution from channel 2.
4. Best fit translational energy  $P(E)$  and center-of-mass angular distribution  $T(\theta)$  for the BaO + NO products. Collision energy was 12.5 kcal/mole. Channel 1 represents the channel involving long-lived  $\text{BaNO}_2$  collision complexes and channel 2 is the direct forward scattered channel.
5. BaO product angular distributions obtained at mean collision energies of 31 and 59 kcal/mole.

6. Same as Fig. 3 but  $E_{\text{coll}} = 59 \text{ kcal/mole}$ .
7. Same as Fig. 4 but  $E_{\text{coll}} = 59 \text{ kcal/mole}$ .
8. BaO product flux contour map at  $E_{\text{coll}} = 12.5 \text{ kcal/mole}$ . A- Newton diagram B- Contribution from channel 1. C- Contribution from channel 2. C- Total BaO product flux (Channel 1 + Channel 2).
9. BaO product flux contour map for channel 1 + channel 2 superimposed on the nominal Newton diagram.  $E_{\text{coll}} = 12.5 \text{ kcal/mole}$ .
10. BaO product angular distribution at collision energy of  $12.5 \text{ kcal/mole}$  showing effect of electronic excitation of the incident Ba atoms. Laser excitation was at the collision zone. Beam consists of approx. 30%  $^1\text{D}$ , 35%  $^1\text{P}$ , 35%  $^1\text{S}$ . Nominal Newton diagram showing circles representing maximum BaO velocities from reaction of ground state Ba( $^1\text{S}$ ) (dotted line) and electronically excited Ba( $^1\text{P}$ ) (solid line).
11. BaNO product angular distribution at collision energy of  $59 \text{ kcal/mole}$ . Laser off: ●- Experimental points, --- Fit to data. Laser focussed at interaction region: □- Experimental points, — Fit to data. Newton diagram is also shown.
12. BaNO product time-of-flight data from reaction of Ba( $^1\text{S}$ ) at indicated laboratory angles for  $\text{Ba} + \text{NO}_2 \rightarrow \text{BaNO} + \text{O}$ . Collision energy was  $59 \text{ kcal/mole}$ . o- Experimental points. — Fit to data.
13. Same as Fig. 12 but with laser excitation at interaction region.
14. Best fit translational energy  $P(E)$  and center-of-mass angular distribution  $T(\theta)$  for the  $\text{BaNO} + \text{O}$  products. Collision energy was  $59 \text{ kcal/mole}$ . --- Laser off. — Laser excitation at interaction region.
15. Center-of-mass product flux contour map in velocity space for the BaNO product from the  $\text{Ba} + \text{NO}_2$  reaction. Laser is off.  $E_{\text{coll}} = 59 \text{ kcal/mole}$ .
16. Electron probability density maps for the half occupied  $6a_1$  and unoccupied  $2b_1$  orbitals of  $\text{NO}_2$ .
17. Energy level diagram for reaction of  $\text{Ba}(^1\text{S}) + \text{NO}_2$ . Shaded area indicates uncertainties in thermodynamic quantities.

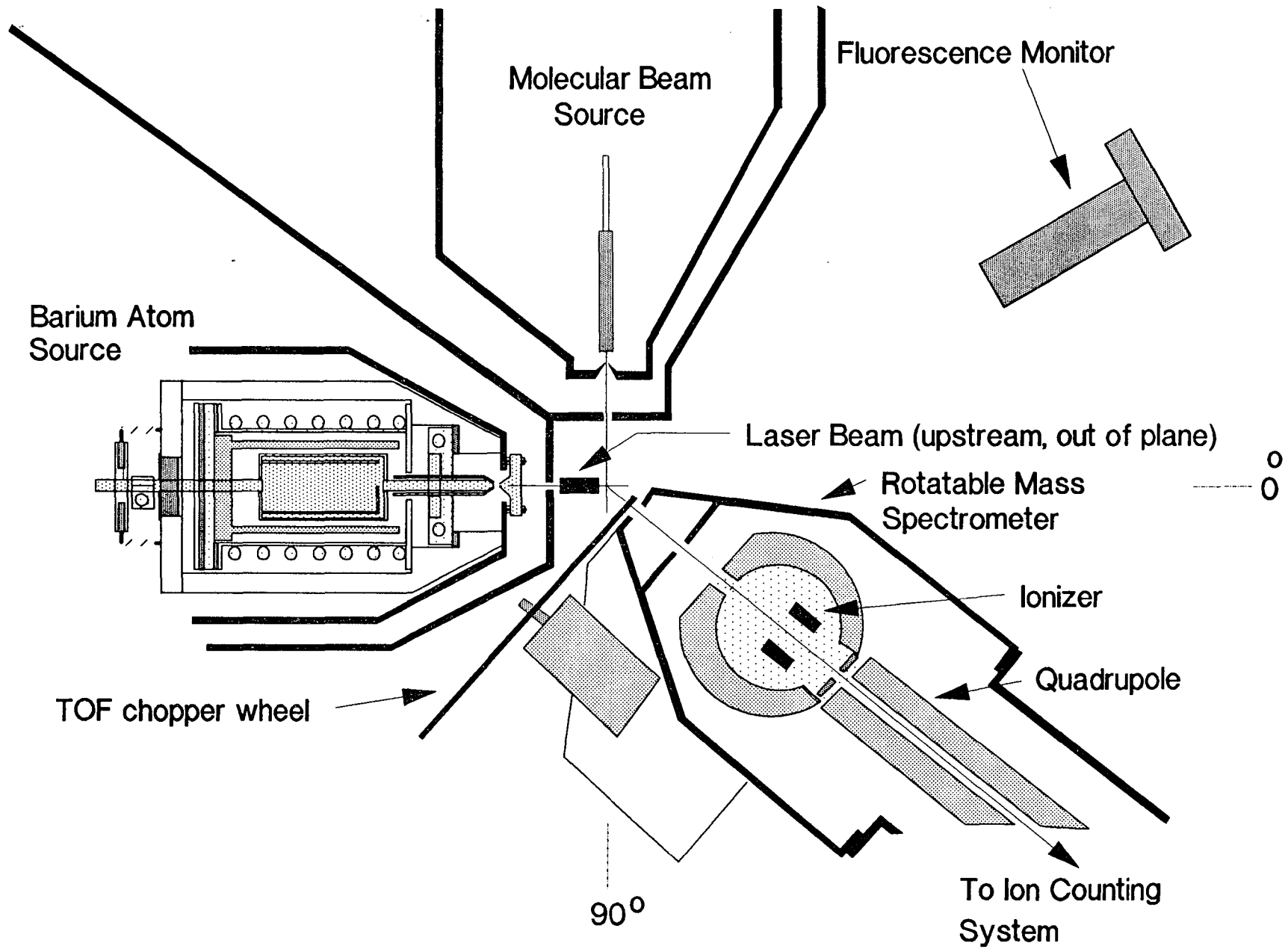


Figure 1

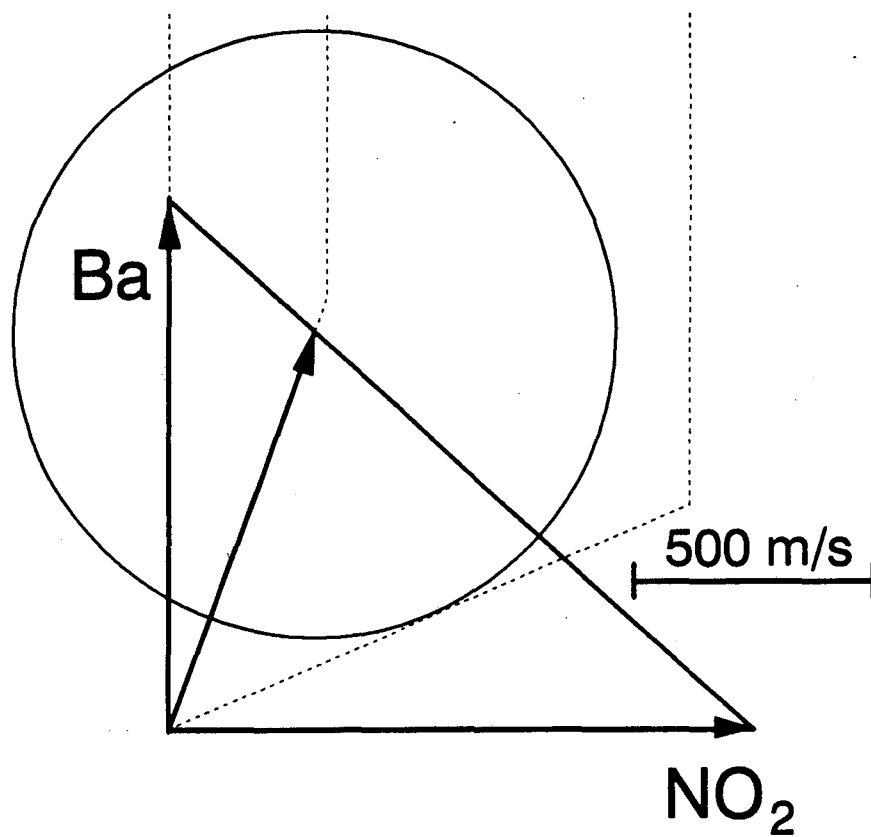
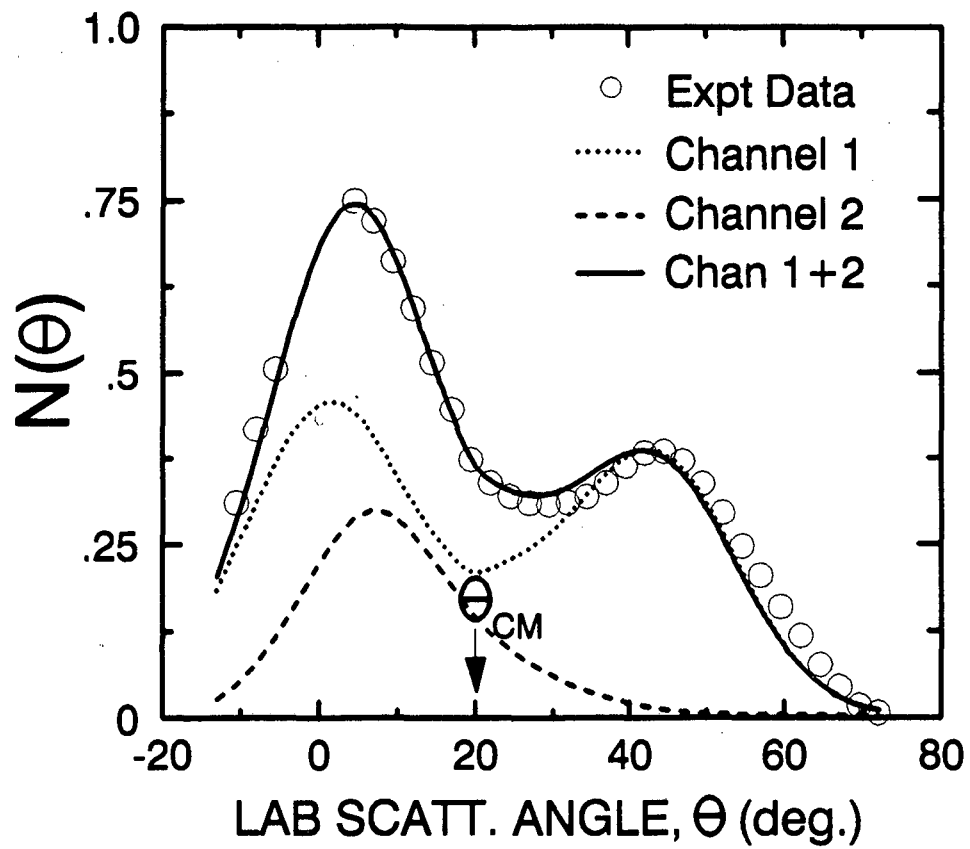


Figure 2

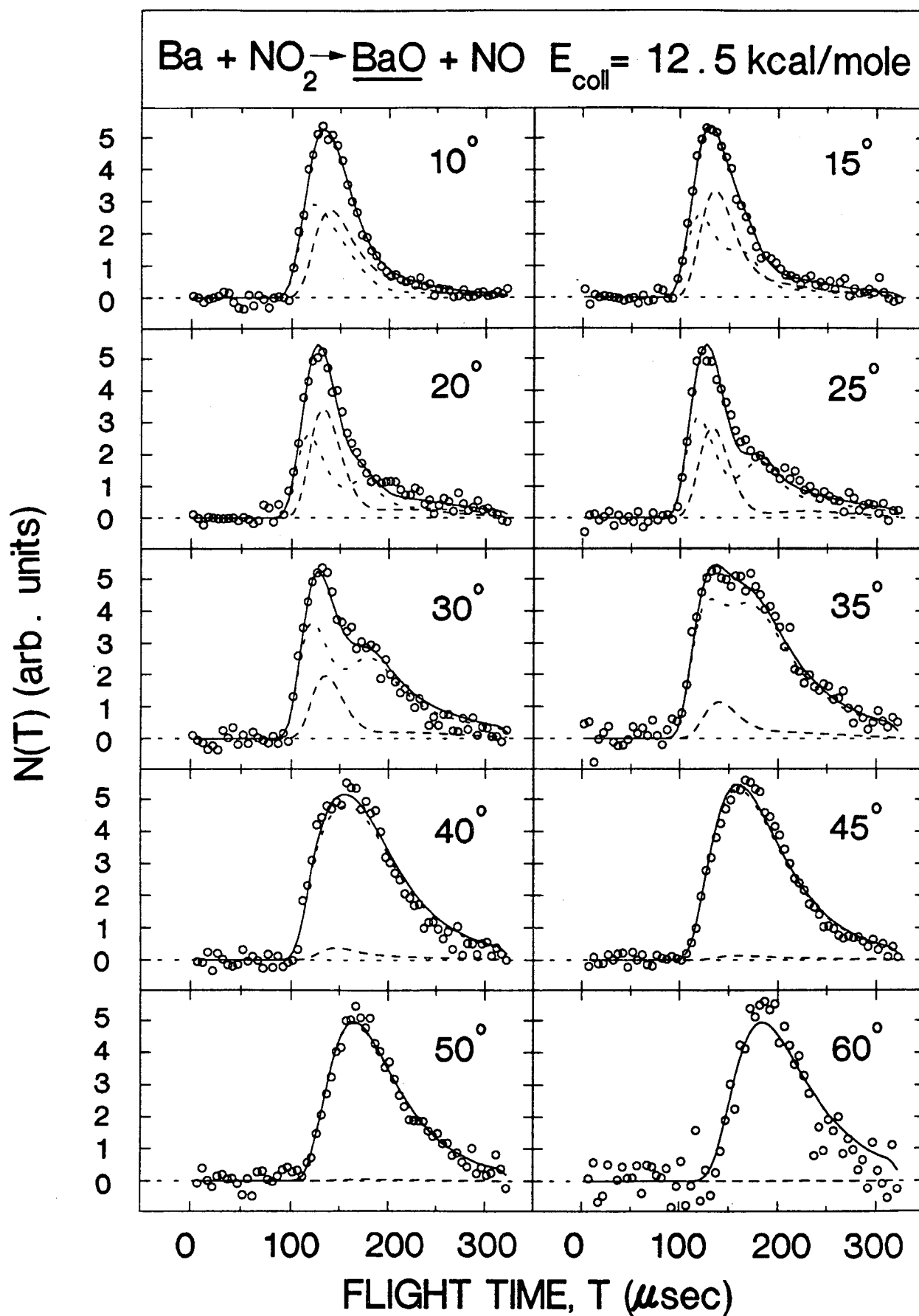


Figure 3

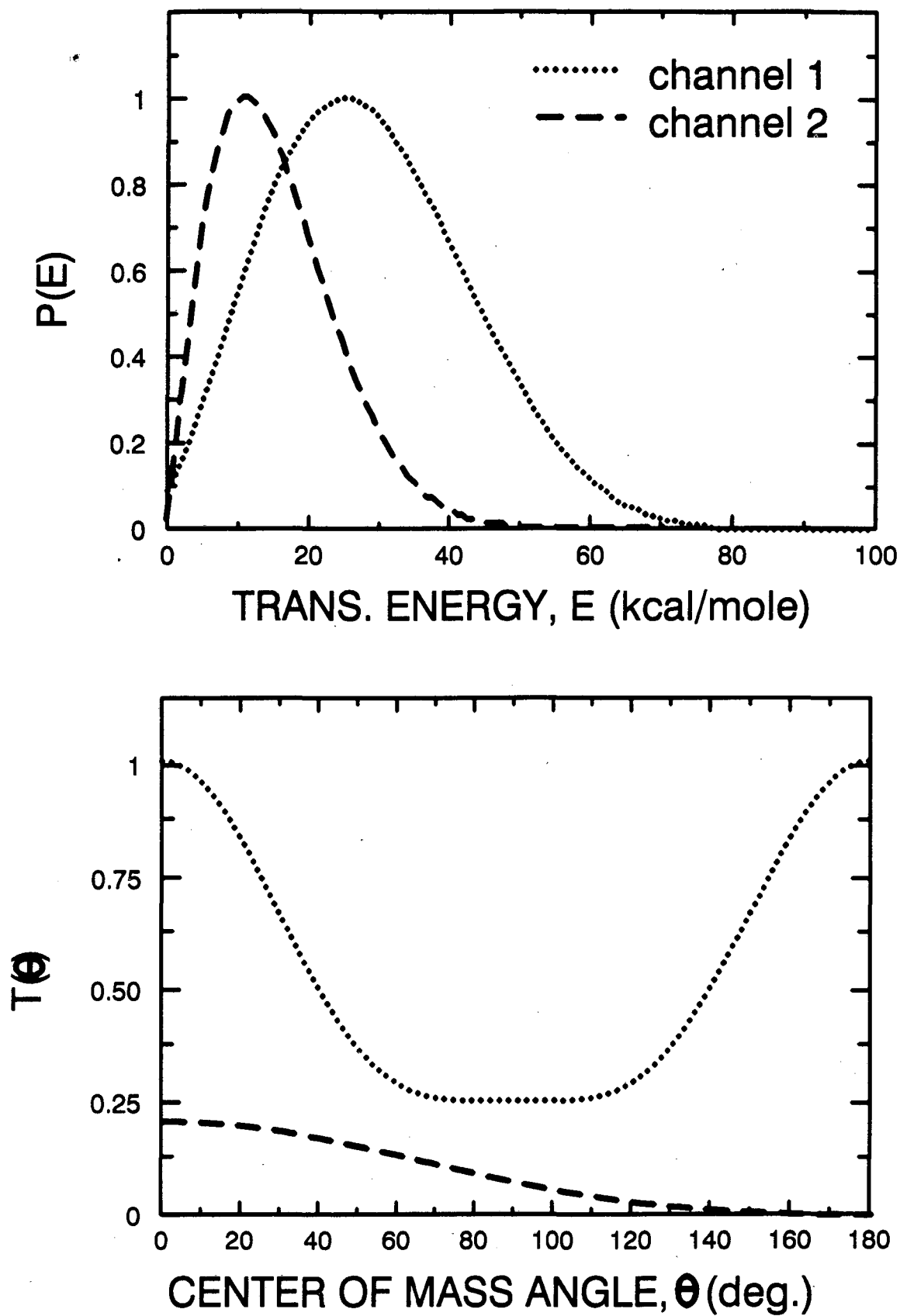


Figure 4

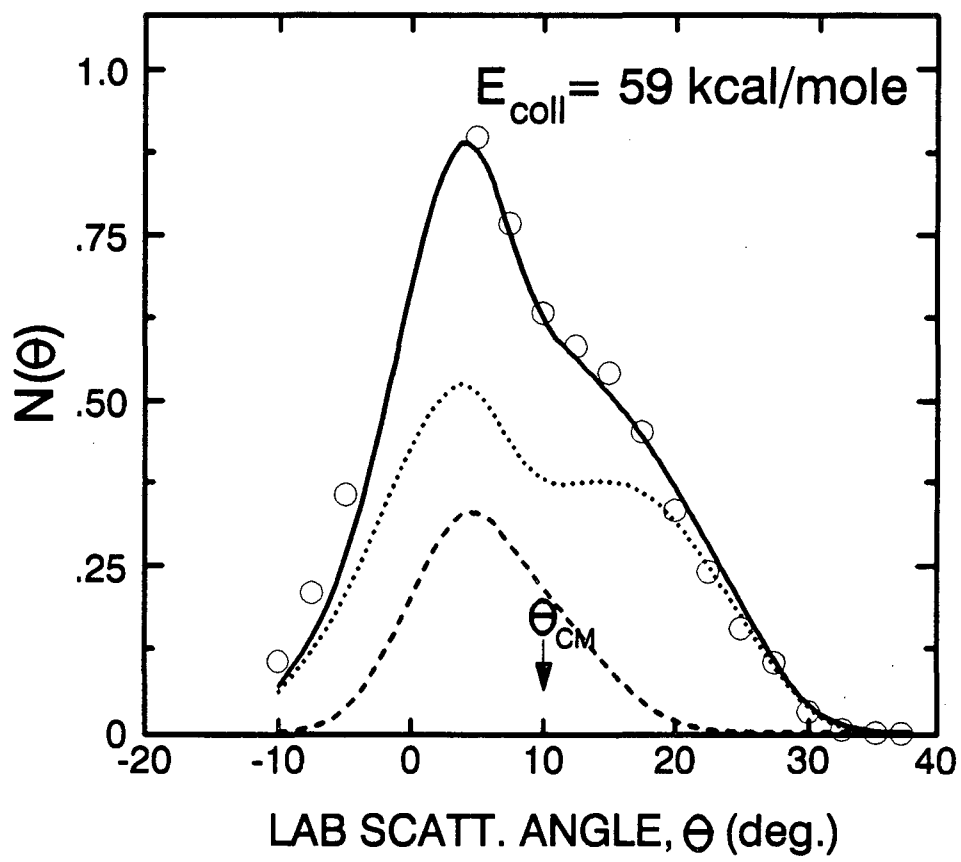
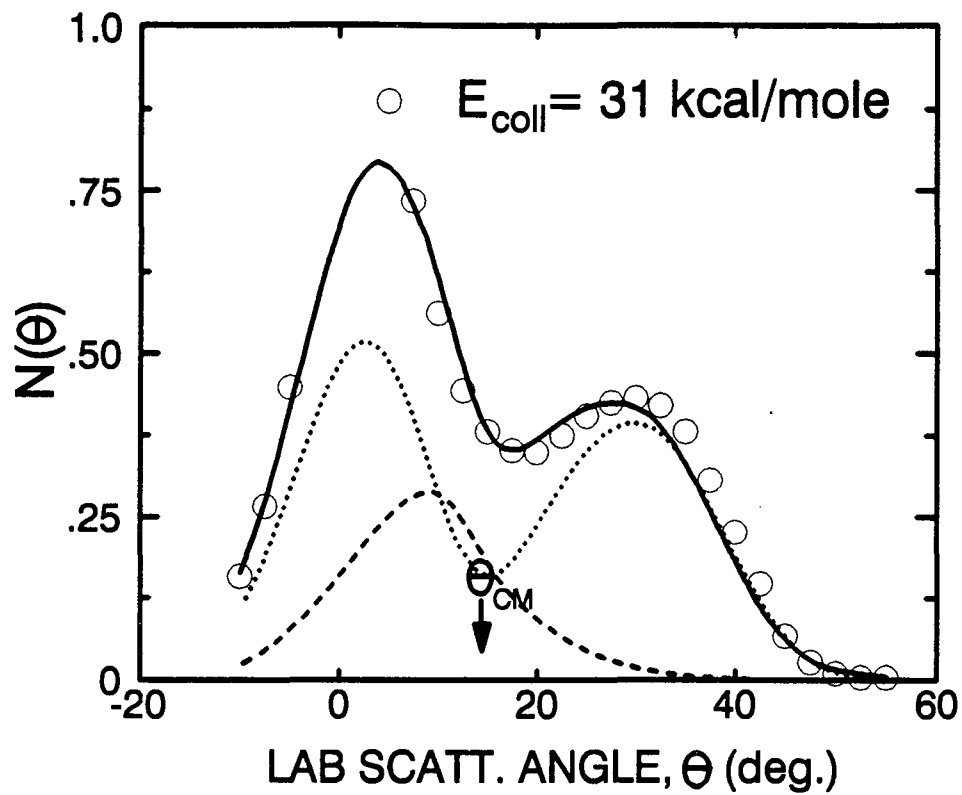


Figure 5

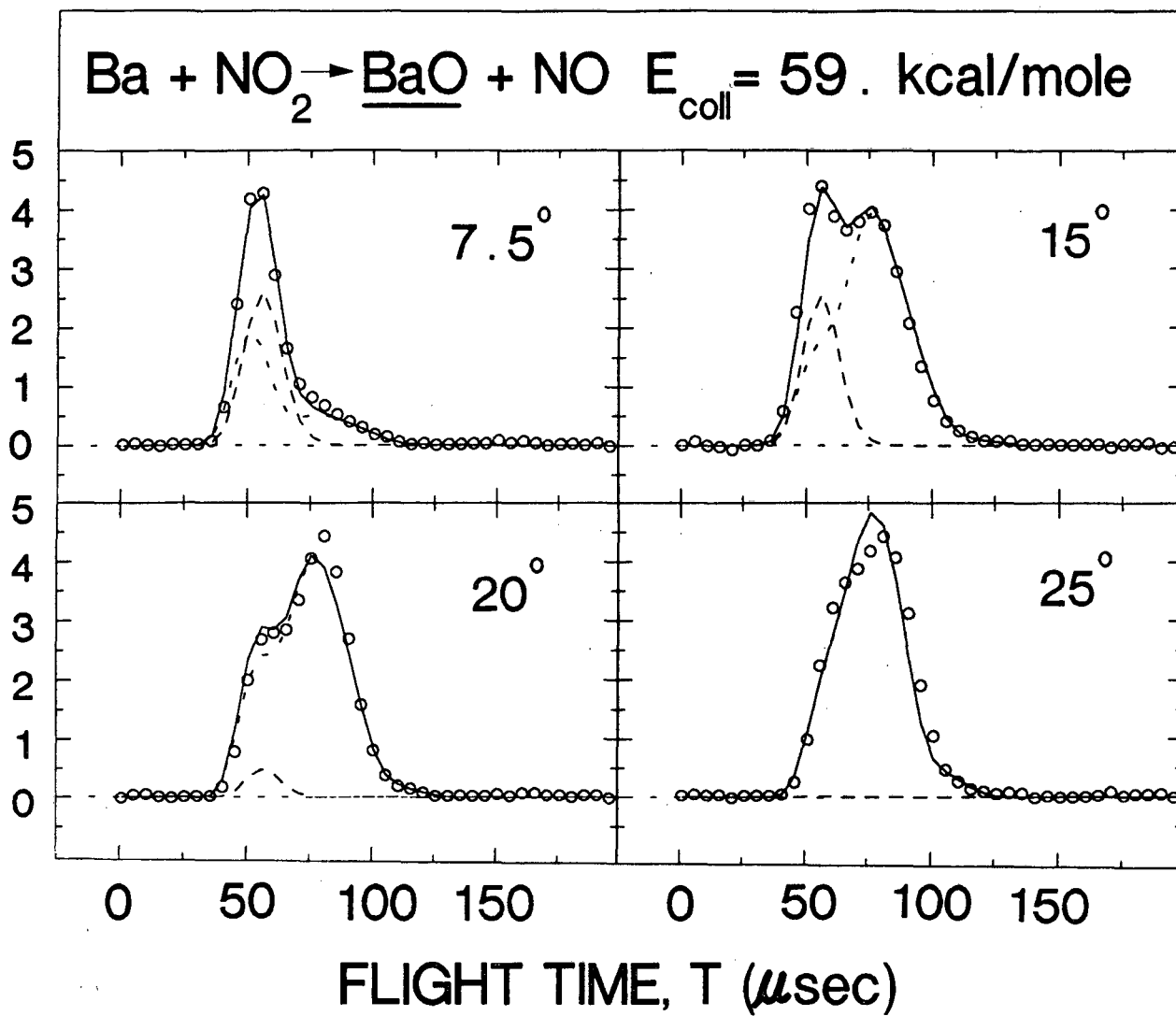


Figure 6

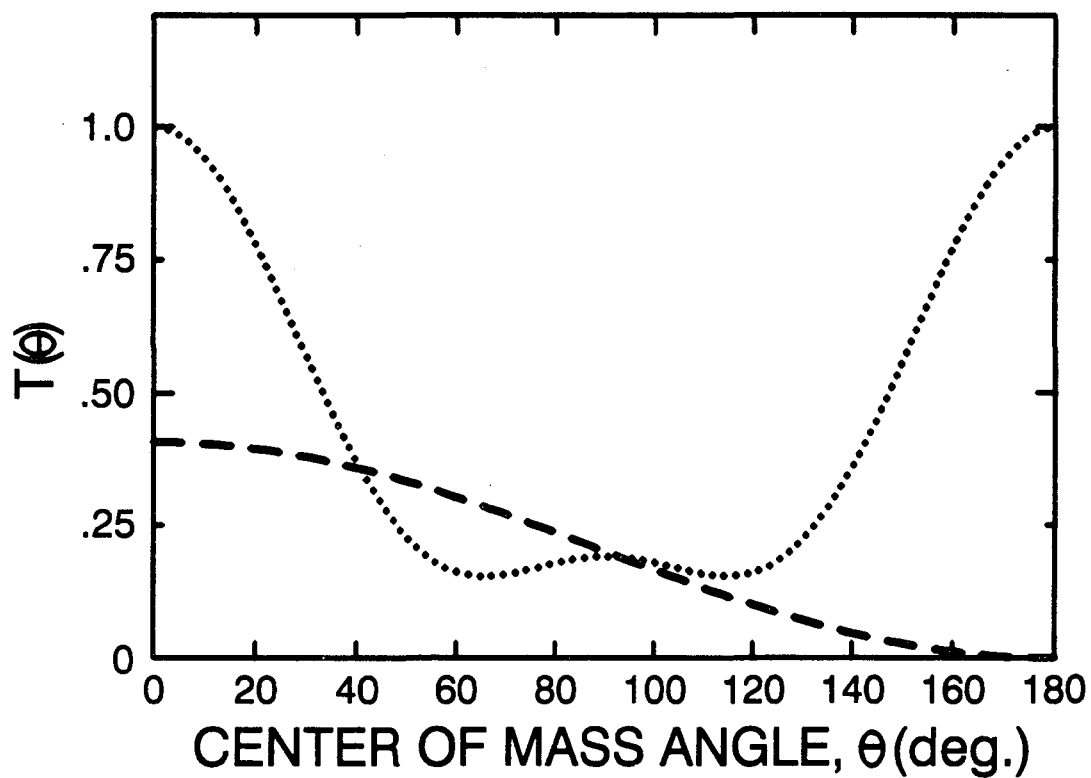
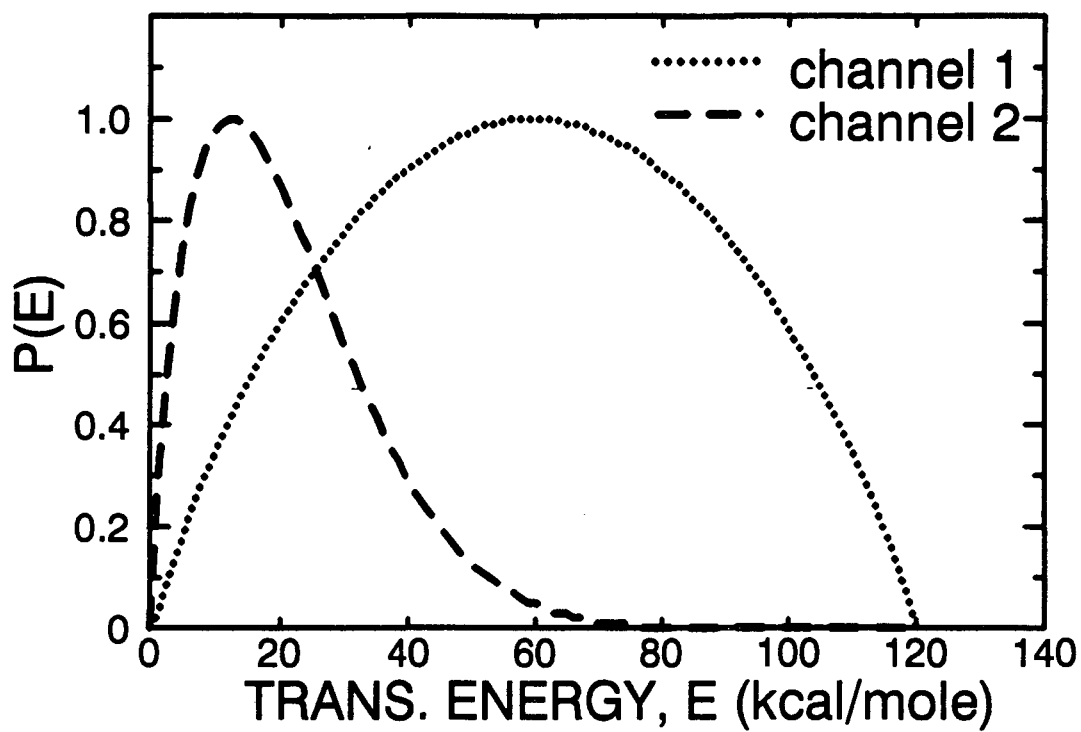


Figure 7

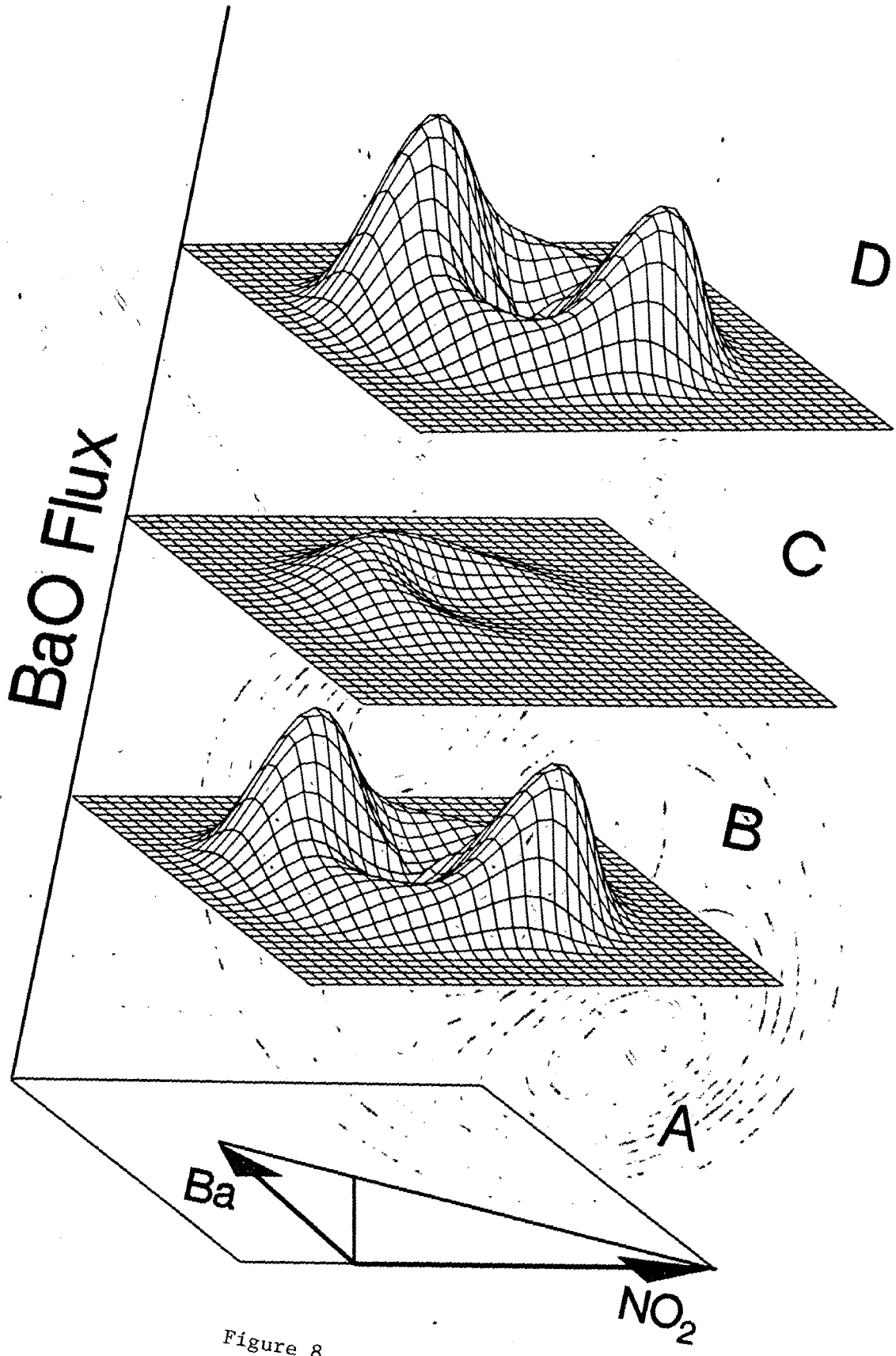


Figure 8

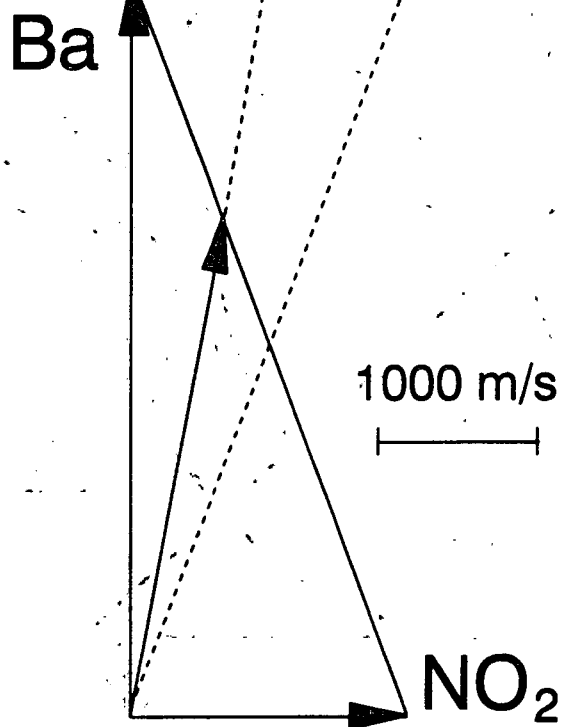
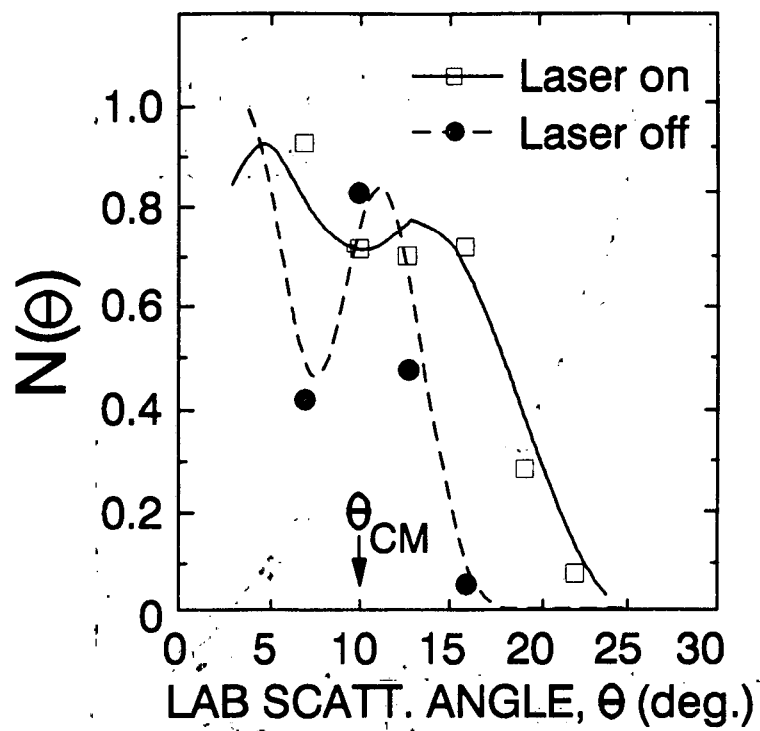


Figure 11

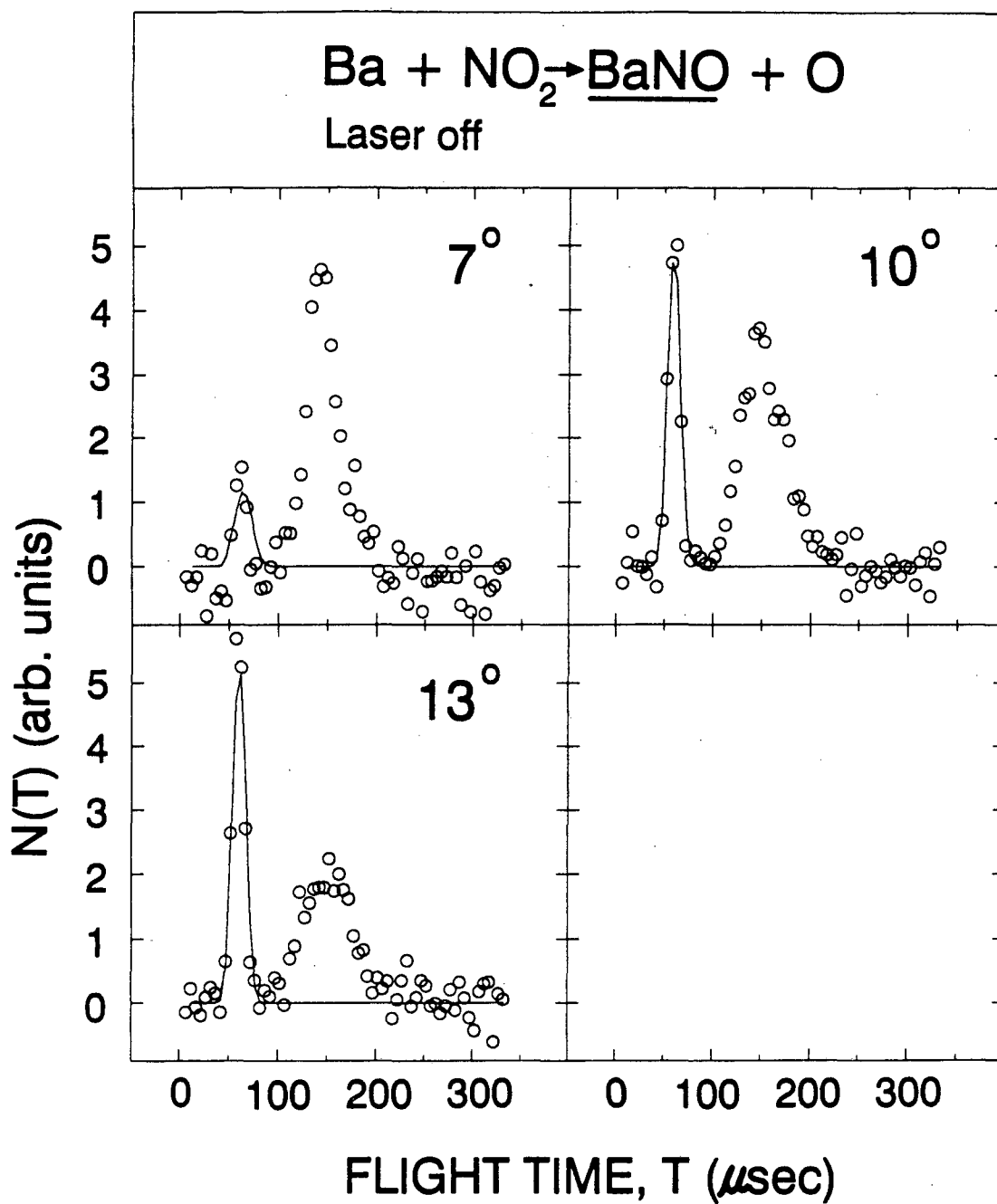


Figure 12

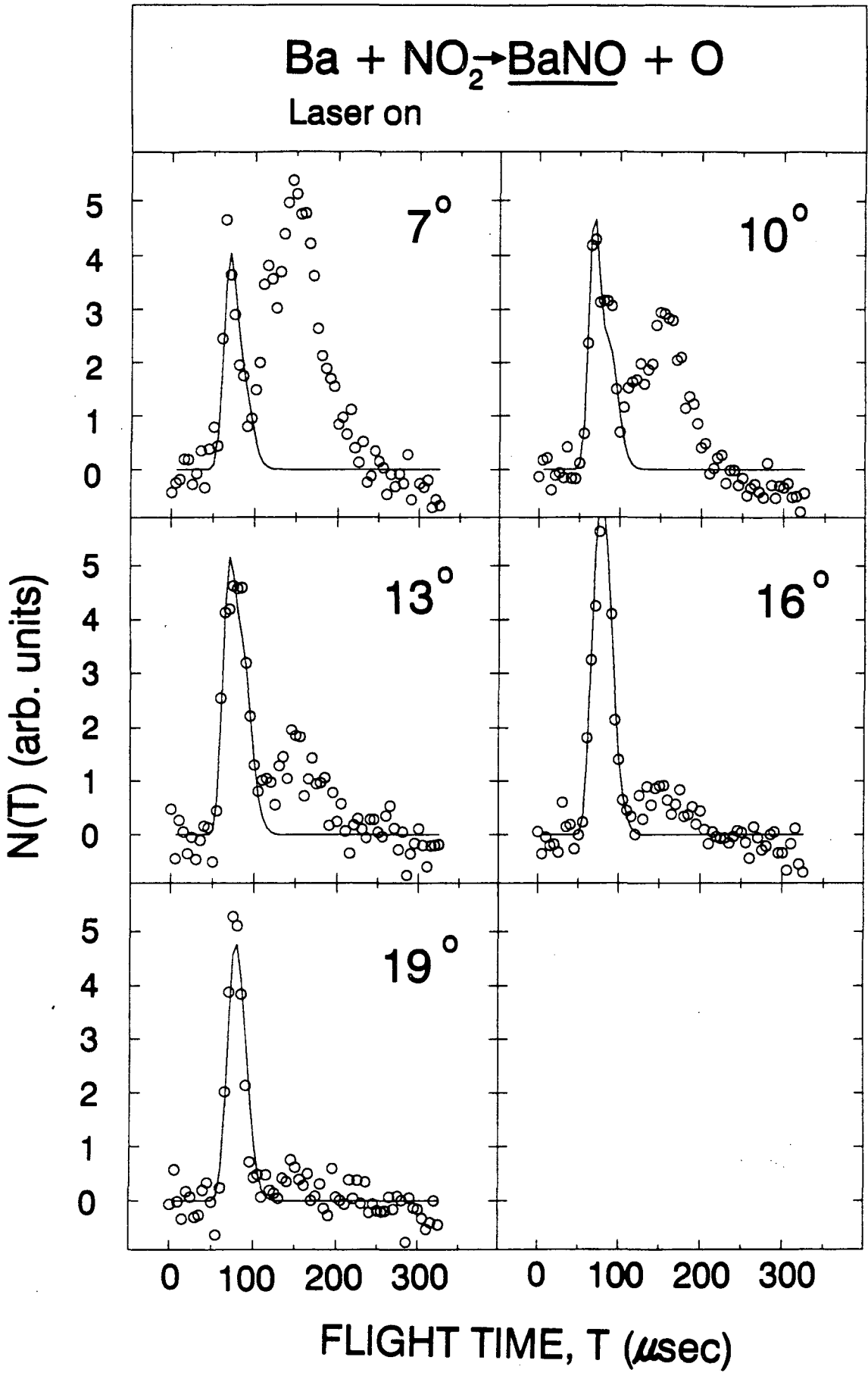


Figure 13

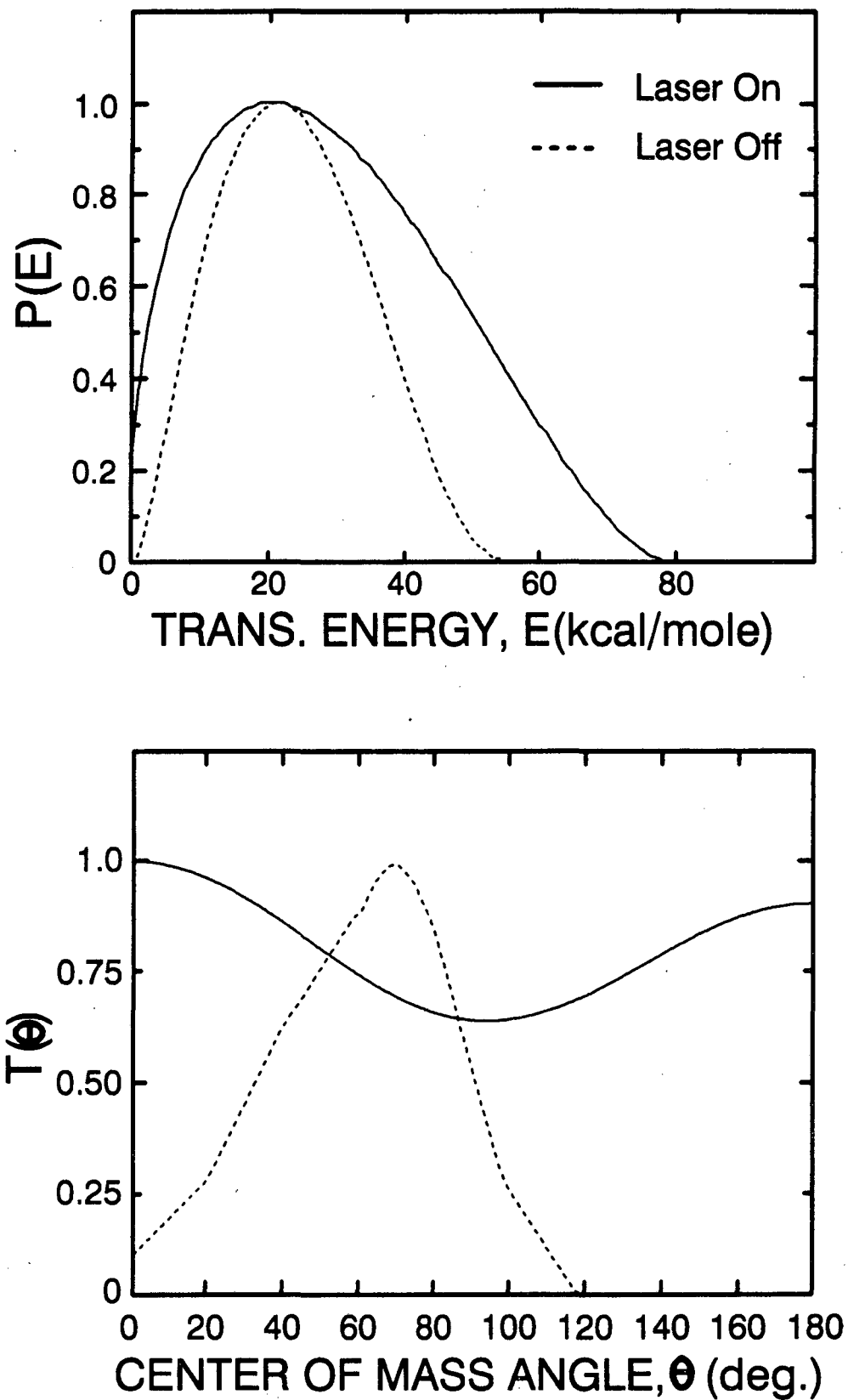


Figure 14

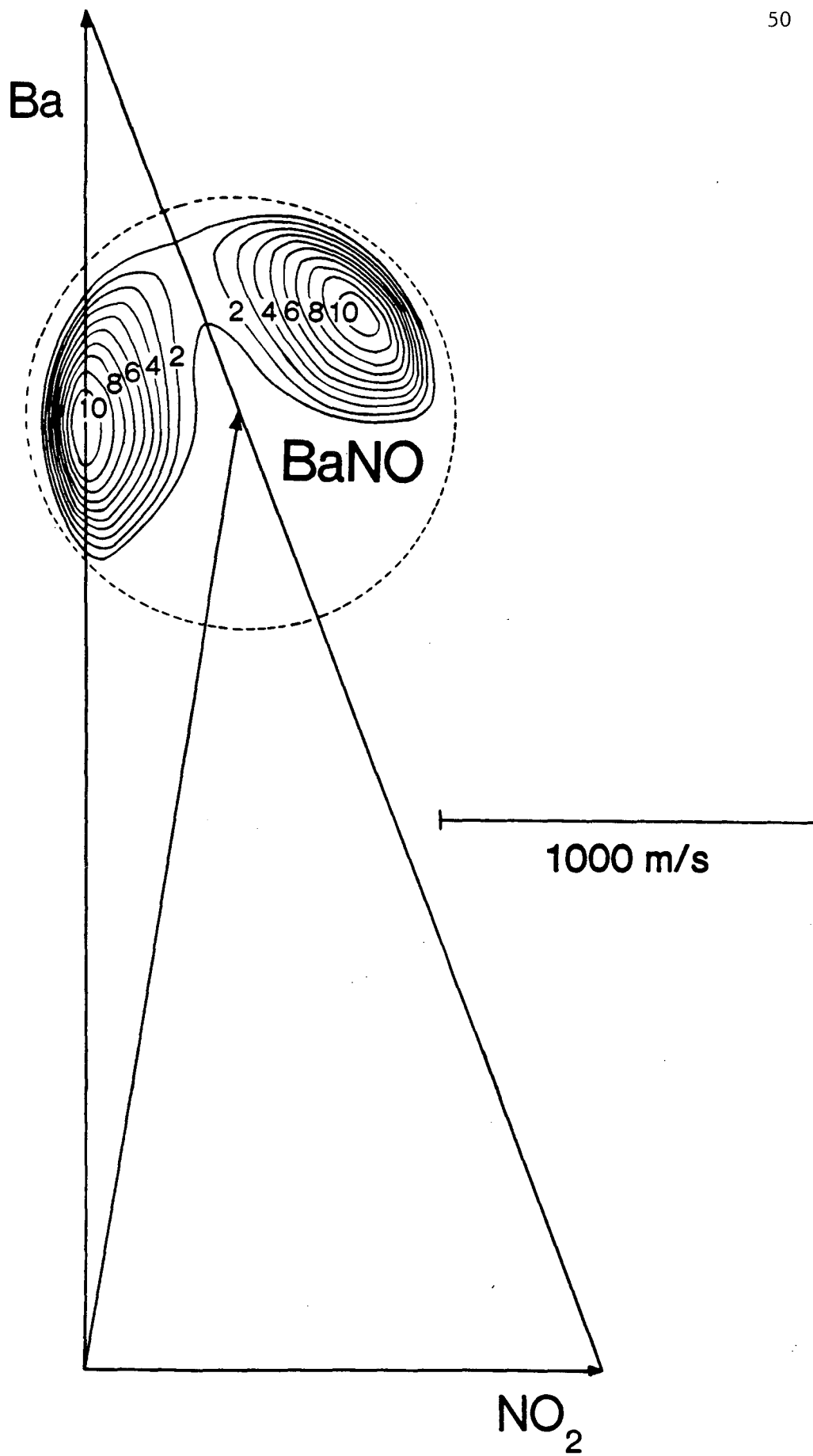


Figure 15

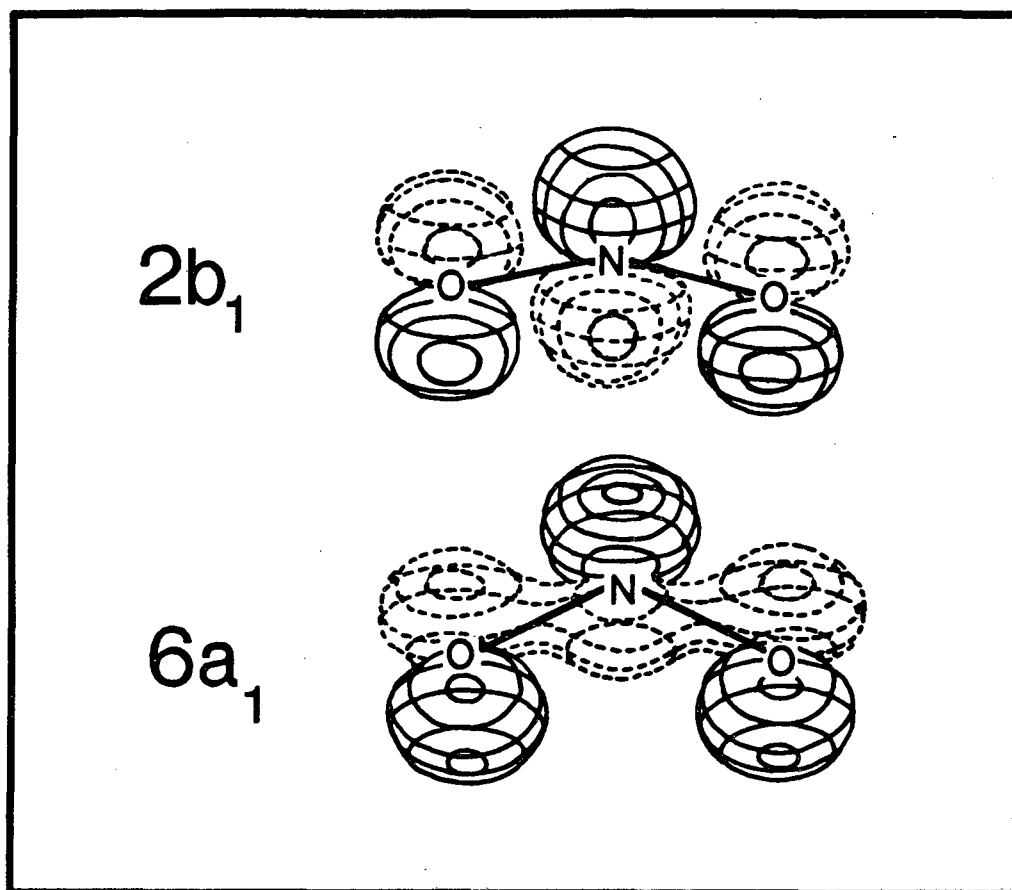


Figure 16

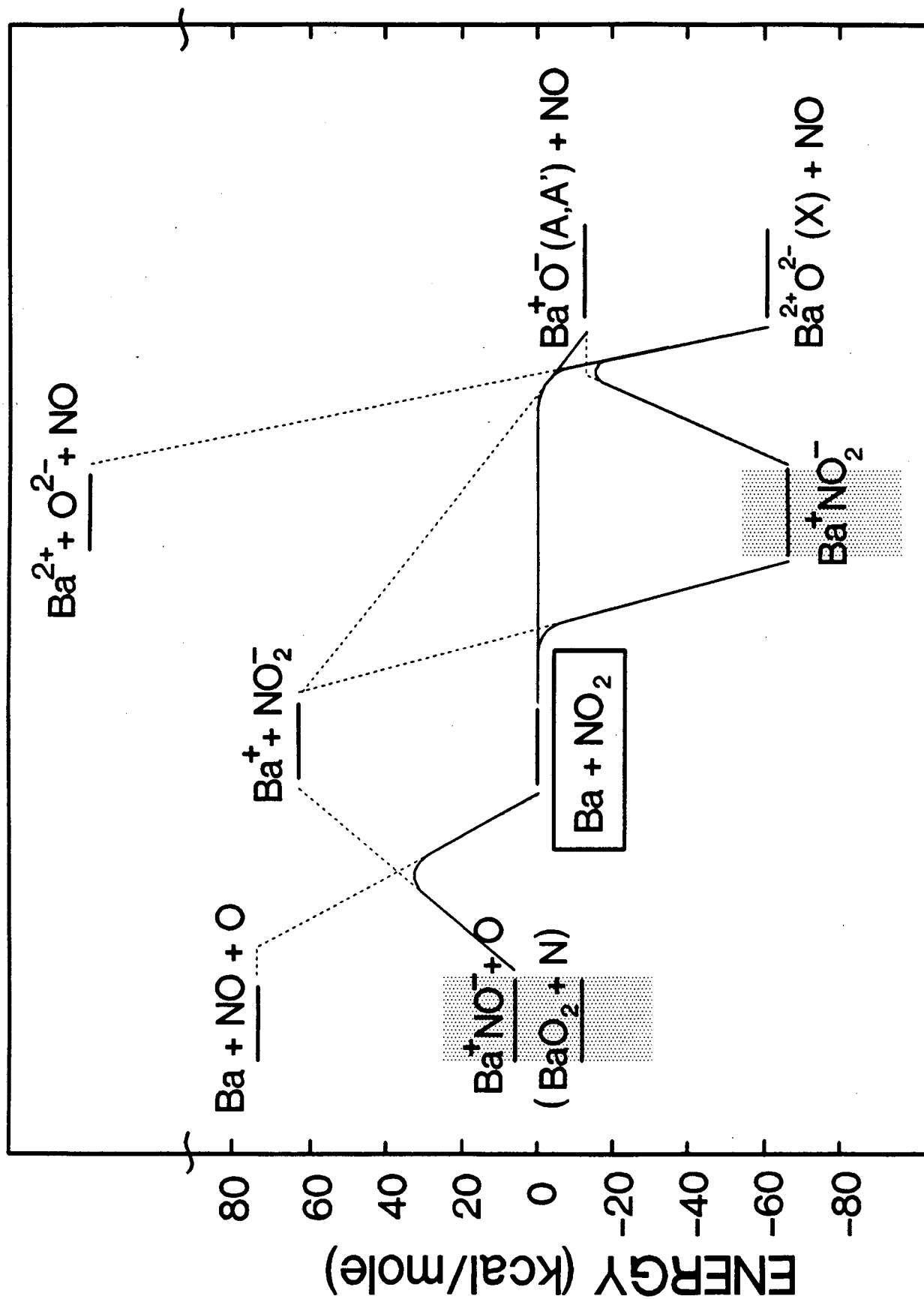


Figure 17

LAWRENCE BERKELEY LABORATORY  
UNIVERSITY OF CALIFORNIA  
INFORMATION RESOURCES DEPARTMENT  
BERKELEY, CALIFORNIA 94720